# Severe reduction Reduction of carbon, alkalinity and nutrient fluxes in the southern Baltic Sea caused by dragging of otter trawl nets across the seafloor

- Pankan Linsy <sup>1</sup>, Stefan Sommer <sup>1</sup>, Jens Kallmeyer <sup>2</sup>, Simone Bernsee <sup>2</sup>, Florian Scholz <sup>3</sup>, Habeeb Thanveer Kalapurakkal <sup>1a</sup>, Andrew W. Dale <sup>1</sup>
  - <sup>1</sup> GEOMAR Helmholtz Centre for Ocean Research Kiel, Wischhofstraße 1–3, 24148 Kiel, Germany
  - <sup>2</sup>GFZ Helmholtz Centre for Geosciences, Telegrafenberg, 14473 Potsdam, Germany
  - <sup>3</sup> Institute for Geology, Center for Earth System Research and Sustainability, Universität Hamburg, Hamburg, Germany.
    - <sup>a</sup> Now at: Alfred Wegener Institute Helmholtz Centre for Polar and Marine Research, 27570 Bremerhaven, Germany

Correspondence to: Pankan Linsy (linsyp@geomar.de)

15

10

## **Abstract**

Bottom trawling Mobile bottom-contacting fishing (MBCF) represents a substantial anthropogenic disturbance, 20 significantly disrupting seafloor integrity and altering oceanic carbon storage. In this study, we conducted a benthic trawling experiment on organic-rich muddy sediments in the Mecklenburger Bight, southern Baltic Sea, employing an otter trawl. Multiple trawl tracks were made to assess the temporal impact of bottom fishing on the benthic ecosystem over time scales ranging from days to weeks. Focus was on the wide area where the net footrope was dragged between the otter boards, rather than on much smaller area impacted by the trawl doors. This study 25 constitutes the first comprehensive investigation to systematically monitor the effects of bottom trawlingMBCF on benthic oxygen, carbon, alkalinity and nutrient fluxes using autonomous in situ lander measurements. Seafloor observations revealed a profound impact of trawling on seafloor morphology. Flux measurements, coupled with sediment data, indicated reductions in benthic fluxes of O2, dissolved inorganic carbon (DIC), total alkalinity (TA), and nutrients (PO<sub>4</sub><sup>3-</sup>, NH<sub>4</sub><sup>+</sup>, and H<sub>4</sub>SiO<sub>4</sub>) within trawled areas compared to control sites. Additionally, 30 observed decreases in organic carbon remineralization rates suggest that bottom trawlingMBCF alters benthic respiration by disrupting key biogeochemical processes. Fluxes of O2, DIC, and TA had not returned to baseline levels by the conclusion of the 16-day observation period, indicating prolonged disturbance effects, although natural temporal variations may have an influence. Despite substantial alterations to the benthic biogeochemical pathways, modeling suggests that the reduction in benthic DIC and TA fluxes exerts only a minor influence on 35 CO<sub>2</sub> release to the atmosphere compared to the much larger potential impact of pyrite oxidation in resuspended sediment.

# 1. Introduction

40

45

Bottom trawling (mobileMobile bottom-contact-contacting fishing (MBCF) is one of the major anthropogenic activities that significantly affect the marine environment (Depestele et al., 2019; Hiddink et al., 2006; Oberle et al., 2016b; Olsgard et al., 2008; Pusceddu et al., 2014). Trawling involves catching benthic and demersal fish by towing nets along the seafloor using various devices. Bottom trawling gearMBCFgear can penetrate the seafloor and dislocate the sediment to varying depths depending on the sediment type and gear used (Martín et al., 2014). Approximately 4.9 million km² or 1.3% of the global ocean is estimated to be trawled each year (Sala et al., 2021). The impacts of bottom trawlingMBCF include the alteration of seabed morphology through the scraping, ploughing, and resuspension of surface sediments (Bruns et al., 2023; Oberle et al., 2016b). These processes ultimately disrupt benthic biogeochemical cycles (Allen and Clarke, 2007; Bradshaw et al., 2021; Bruns et al., 2023; Hale et al., 2017; Morys et al., 2021; Sciberras et al., 2016; Tiano et al., 2019; van de Velde et al., 2018). Additionally, bottom trawlingMBCF has been shown to significantly reduce benthic fauna biomass (Bergman,

50 2000; Bergman and Meesters, 2020; Tiano et al., 2022) and, ultimately, change benthic community structures (Bradshaw et al., 2024; Kaiser et al., 2002; Pusceddu et al., 2014).

55

60

65

70

75

80

85

90

95

100

The seafloor disturbance caused by trawling has been argued to disrupt oceanic carbon sequestration (Atwood et al., 2024; Epstein et al., 2022; Hiddink et al., 2023; Sala et al., 2021; Zhang et al., 2024) as marine sediments serve as a critical reservoir for long-term carbon storage (Burdige, 2007; LaRowe et al., 2020). The study by Sala et al., (2021) suggests that seafloor disturbances caused by trawling and dredging result in the annual release of 0.58-1.47 Pg of CO<sub>2</sub>, largely due to increased remineralization of particulate organic carbon (POC). Atwood et al. (2024) estimated that 50-60% of the CO2 released due to trawling is emitted into the atmosphere over a decade, accounting for approximately 0.34–0.37 Pg CO<sub>2</sub> per year globally. In particular, trawling in shelf seas has been shown to reduce POC by 29% (Porz et al., 2024), with long-term losses equivalent to emissions of 3.67 Mg CO<sub>2</sub> km<sup>-2</sup> yr<sup>-1</sup>, assuming complete mineralization of the disturbed POC (Zhang et al., 2024). However, a subsequent metadata analysis by Epstein et al., (2022) yielded mixed findings on the impact of trawling on POC stock, revealing no significant effect in 61% of the 49 studies analyzed. Among the remaining studies, 29% reported decreased POC levels associated with fishing activities, while 10% observed an increase in POC. These results indicate that the impact of bottom trawling MBCF is site-specific and probably influenced by factors such as trawling frequency, type of fishing gear, local lithology, and towing intensity (De Borger et al., 2021; Depestele et al., 2019; Oberle et al., 2016a; Tiano et al., 2019). Thus, site-specific studies are necessary for studying the impact of bottom trawling MBCF in any given region (Stephens and McConnaughey, 2024).

Bottom fishing is carried out over large swathes of the Baltic Sea (HELCOM, 2018), and approximately 36% of the seafloor in the southwestern Baltic Sea is affected (Díaz-Mendoza et al., 2025). A study by Van Denderen et al. (2020) revealed that trawling, together with bottom water hypoxia, has led to a 50 % reduction in benthic biomass in 14% of the Baltic Sea region. The impact of bottom trawling MBCF on the benthos in the Baltic Sea has been the subject of numerous studies (Bradshaw et al., 2021, 2024; Bunke et al., 2019; Corell et al., 2023; Morys et al., 2021; Porz et al., 2023; Rooze et al., 2024; Schönke et al., 2022), but relatively few have examined the impact on benthic biogeochemistry (Bradshaw et al., 2021, 2024; Morys et al., 2021; Rooze et al., 2024; Tiano et al., 2024). Morys et al. (2021) conducted a controlled benthic dredging experiment in previously untrawled regions of the Baltic Sea. The experiment simulated the sediment disturbance caused by trawl gears by removing the surface sediment, allowing for a comparative analysis of geochemical characteristics with an adjacent pristine area. Immediate post-disturbance observations indicated alterations in benthic nutrient fluxes and porewater profiles. Bradshaw et al., (2021) conducted a controlled field experiment in muddy sediments of the Baltic Proper using a commercial otter trawl to quantify the physical and biogeochemical impacts of bottom trawling. MBCF. Their findings indicated a reduction in oxygen penetration depth into the seafloor as well as altered nutrient and oxygen fluxes across the sediment-water interface. The trawl track persisted for at least 18 months, which suggests that sediment biogeochemistry may not fully recover in areas with frequent bottom trawling. MBCF. However, as a single-track experiment, these findings may not fully represent the cumulative impacts of trawling, particularly in areas where bottom trawling MBCF occurs intensively more than 10 times per year (HELCOM, 2018).

When examining the impact of trawling activities on the oceanic carbon pool, it is also crucial to consider the effects of trawling on sedimentary total alkalinity (TA) and dissolved inorganic carbon (DIC) fluxes rather than solely focusing on organic carbon remineralization. Sediment-water reactions influence the ocean's buffering capacity, thereby affecting its ability to take up CO<sub>2</sub> from the atmosphere (Zeebe and Wolf-Gladrow, 2001). In the continental shelf ecosystem, in addition to the burial of organic carbon, benthic alkalinity production plays a key role in net carbon sequestration (Van Dam et al., 2022). The shallowness of coastal seas further permits a close interaction between sediments and the atmosphere (Brenner et al., 2016; Burt et al., 2016). Several processes control alkalinity generation in sediments and fluxes to the water column, such as mineral formation and dissolution, denitrification, pyrite formation and burial, and reverse weathering (Hu and Cai, 2011; Krumins et al., 2013; Middelburg et al., 2020). Among these, alkalinity production associated with pyrite formation likely constitutes a significant blue carbon sink (Hu and Cai, 2011; Reithmaier et al., 2021). Experimental and modeling studies have shown that trawling-induced resuspension reduces the capacity of the Baltic Sea to remove atmospheric CO<sub>2</sub> by decreasing alkalinity, mainly through the oxidation of pyrite (Kalapurakkal et al., 2025). More broadly, bottom trawling MBCF and dredging activities are estimated to reduce alkalinity generation, thereby weakening the marine carbon sink by approximately 2-8 Tg CO<sub>2</sub> per year, through their impact on both organic and inorganic carbon cycling (van de Velde et al., 2025). The field observations conducted to date have not specifically investigated the impact of bottom trawling MBCF on alkalinity fluxes. Therefore, additional fieldbased investigations are essential to comprehensively understand the influence of bottom trawlingMBCF on the broader carbon cycle in addition to the associated biogeochemical upheavals at the sediment surface.

105 As a step toward addressing these critical knowledge gaps, we conducted a benthic trawling experiment in Mecklenburger Bight within the German Exclusive Economic Zone (EEZ) of the Baltic Sea. An otter trawl was deployed to create multiple trawl tracks. Subsequently, dissolved oxygen, DIC, TA, and nutrient fluxes were measured in situ using benthic landers to assess the effect of trawling on sediment regeneration rates, as well as a detailed survey of sediment biogeochemical parameters in recovered sediment cores. Due to low probability of 110 deploying large gears directly on the trawl marks gouged out of by the otter boards, we chose to target instead the much wider net area between the trawl boards (termed the 'net zone'). In addition to the benthic working program, we carried out seafloor imaging to observe the degree of disturbance and redistribution of sediments possibly affecting benthic communities. The major aim of the fieldwork was to determine the direct effects of bottom trawlingMBCF on the benthic ecosystem on time scales of days to weeks and the regeneration capacity of 115 sediment biogeochemistry. We also explored how changes to benthic TA and DIC fluxes impact air-sea CO2 exchange. Our results provide novel insights into trawling-induced alterations in benthic biogeochemical processing in coastal environments.

## 2. Materials and Methods

125

130

# 120 2.1 Study area and experimental strategy

The research cruise AL616 on RV Alkor was undertaken from 18 July to 9 August 2024 in the German EEZ of the Baltic Sea (Sommer et al., 2025). The cruise was embedded in a larger campaign further addressing effects of trawling on different size classes of benthic communities (macrobenthos, meiofauna, protozoans and bacteria/archaea), including sedimentological investigations. Aside from RV Alkor, four research vessels participated in this trawling experiment. On RV Elisabeth Mann Borgese (cruise EMB 345), sediments were sampled for biological analyses. Scientists on the RV Clupea (cruise #389) carried out the trawling and investigated the effects of trawling on fish populations. SCUBA diving operations were performed using the RV Limanda, and the small tender Klaashahn was used to survey the seabed using hydroacoustics. Trawling operations were conducted using a standardized bottom trawl commonly employed in Baltic demersal surveys (TV-3#520x80 mesh size). The gear was equipped with Thyborøn Type 2 Standard trawl doors, each with a surface area of 1.78 m² (Fig. S1). The distance between the otter boards on either side of the trawl net was approximately 60 meters (ICES, 2017). Sediment disturbance within the net area results from interactions with the back strop, sweep lines, chains, bridles, foot rope, and fishing line (see Fig. S1).

The working area was located in the Mecklenburger Bight (southwestern Baltic Sea) 5 km offshore the town of Kühlungsborn at water depths of ~23 m (Fig. 1). It comprises the High-Impact (HI) area with dimensions of 1950 x 300 m that was trawled several times in an east – west direction on 20 July 2024. A Control area (CL) of similar size where no trawling was performed was located west of the HI area. The sediments across the working area were fine-grained muds.

150

155

160

165

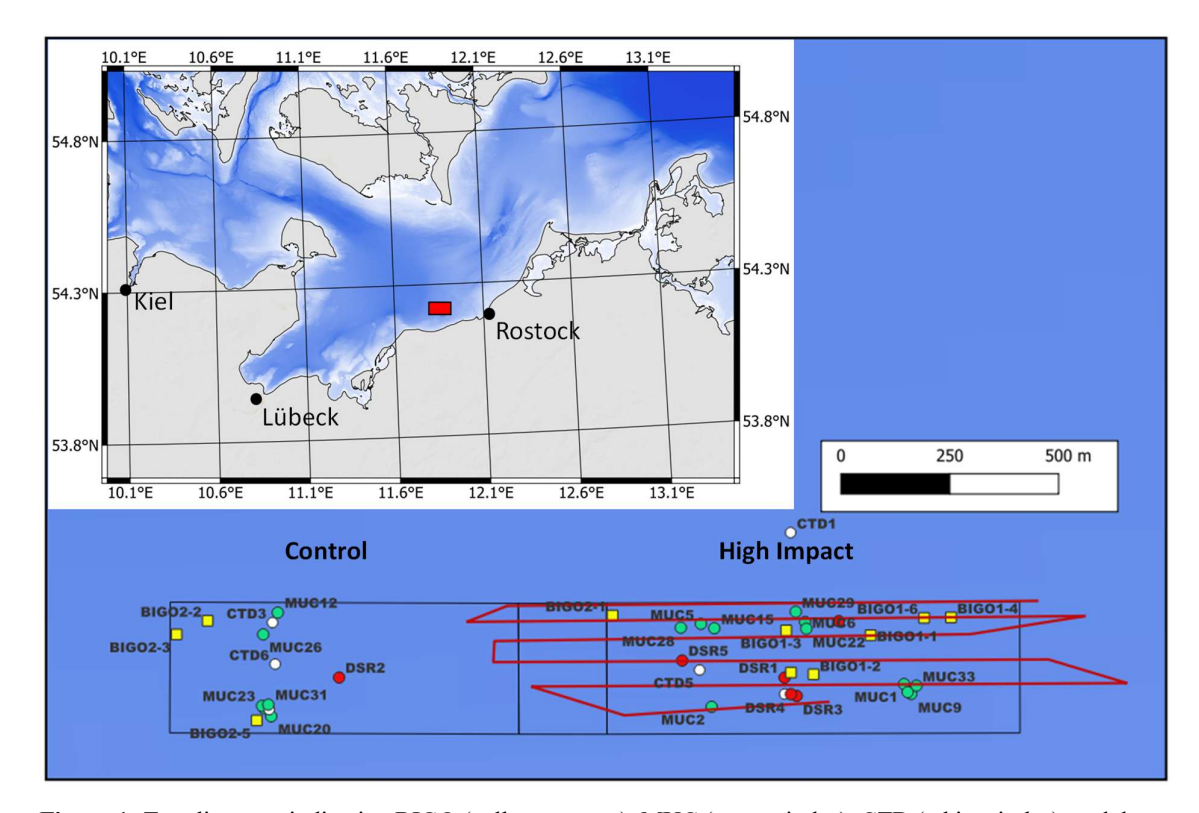


Figure 1: Trawling area indicating BIGO (yellow squares), MUC (green circles), CTD (white circles), and deepsea rover (DSR) (red circles) deployment sites. Red lines indicate trawl tracks. The inset shows the sampling area (red box) in the western Baltic.

## 2.2 Water and sediment sampling

A Sea-Bird Scientific CTD (SBE 9) equipped with a 12-Niskin bottle water sampling rosette was utilized for in situ measurements of salinity, temperature, depth and chlorophyll-a and for retrieving water samples. Data acquisition was performed using Sea-Bird Seasave software (v7.26.7). A total of seven CTD casts were conducted, with three deployments in the CL and HI areas and one outside. Water samples for dissolved oxygen measurement were immediately analyzed onboard using the Winkler method. Samples for nutrient analysis were collected and analyzed onboard.

Sediment samples were collected using a multiple-corer (MUC) with 6 and 11 deployments in the CL and HI areas, respectively (Table S1). Two cores (MUC1 and MUC2) were collected from the HI area prior to the trawling experiment and are considered control samples. The MUC was equipped with seven plastic liners, each 60 cm in length and 10 cm in internal diameter. The MUC was lowered toward the seafloor at a speed of 0.3 m s<sup>-1</sup> in every deployment. Upon reaching the seafloor, lead weights applied gravitational force to drive the liners into the sediment, with a maximum penetration depth of 35 cm. Upon retrieval, all cores were moved to a cooling laboratory maintained at 10°C, which approximates the bottom water temperature at the sampling sites. The cores were sectioned at a resolution of 1 cm near the surface, increasing to 4 cm for sediment depths greater than 20 cm. For all measurements and sub-sampling for redox-sensitive parameters from the MUC cores, the sediments were sectioned inside an argon-filled glove bag to prevent contact with atmospheric oxygen and filled into 50 ml Falcon tubes. Porewater was extracted by centrifuging the samples at 4000 rpm for 20 minutes at 3°C in a refrigerated centrifuge, effectively separating the porewater from the particulates. Following a mechanical failure of the centrifuge, porewater was obtained by inserting Rhizon filters (0.2 μm) into pre-drilled holes in the lids of the centrifuge tubes. Porewaters were then extracted under vacuum using 20 ml plastic syringes. All porewater samples were then filtered (0.2 µm cellulose-acetate syringe filters) under argon. Supernatant bottom water samples of the MUC cores were also collected at each station. Additional sediment samples cores were stored at 4°C in pre-weighed airtight containers for porosity and particulate geochemistry analyses.

For quantification of sulfate reduction rates, we used the radiotracer incubation technique of Jorgensen (1978). Three acrylic tubes (24 mm internal diameter, 3 mm wall thickness) were carefully inserted into a single MUC core from the same deployment as for the geochemistry analyses using suction to avoid compaction during insertion. The tubes were removed from the sediment, both ends sealed with rubber stoppers and stored in an incubator at approximate in-situ temperature. At the end of each day, <sup>35</sup>SO<sub>4</sub><sup>2-</sup> radiotracer solution was injected into the cores, from the water-sediment interface down to 20 cm sediment depth. The radiotracer (15 μl volume, activity ca. 200 kBq) was injected in 1 cm intervals through silicone-sealed holes with 2 mm diameter. The cores were then incubated for 24 h in the dark.

After the incubation, the sediment was pushed out of the acrylic tubes and sectioned. A resolution of 1 cm was selected for the first 6 cm, then 2 cm down to 10 cm, followed by 5 cm for subsequent depths down to 20 cm. Each sediment section was placed in a 50 ml centrifuge tube, pre-loaded with 10 ml of 20% zinc acetate solution to fix all hydrogen sulfide and terminate microbial activity. Samples were thoroughly shaken to break up sediment aggregates and then frozen overnight. Further storage and transport to the home lab was done at room temperature.

### 2.3 In situ flux measurements with BIGO landers

180

215

220

185 In situ flux measurements were conducted using two Biogeochemical Observatories (BIGO-I and BIGO-II). The BIGOs were deployed 3 and 7 times in the CL and HI areas, respectively. Each lander had two measurement chambers (C1 and C2) with a diameter of 28.8 cm and an area of 651 cm<sup>2</sup> (Sommer et al., 2009, 2016). Details of lander deployment protocols can be found elsewhere (Sommer et al., 2009, 2016). Sediments were incubated for 30 to 48 hours, and discrete samples (~47 mL) of overlying water were collected at pre-programmed intervals 190 using glass syringes. The glass syringes were connected to the chambers through 1-meter-long Vygon tubes filled with distilled water with a dead volume of 6.9 mL. An additional eight glass syringe water samples were collected to monitor ambient bottom water conditions at the same time intervals. Another sample set was collected for the analysis of DIC and TA in quartz glass tubes. Water samples from the glass syringes were immediately transferred to a cooling laboratory and subsampled for analyses of nitrate (NO<sub>3</sub>-), nitrite (NO<sub>2</sub>-), ammonium (NH<sub>4</sub><sup>+</sup>), phosphate 195 (PO<sub>4</sub><sup>3-</sup>), and silicic acid (H<sub>4</sub>SiO<sub>4</sub>). Oxygen was measured inside the chambers and in the ambient seawater using optodes (Aanderaa). They were two point calibrated before each lander deployment using well-oxygenated seawater and anoxic seawater, which was produced by adding 5 to 15 g of Na<sub>2</sub>S. The dilution error from the distilled water in the glass syringe samples, was corrected using chloride concentrations measured in the syringe samples and the ambient seawater. Nutrient and oxygen fluxes were determined by multiplying slope of the linear 200 regression of the concentration versus time slope by the height of the water inside the chamber. Fluxes determined this way include fluxes by molecular diffusion in addition to non-local transport by bioirrigation and thus constitute the total solute flux. Oxygen fluxes are thus reported as total oxygen uptake (TOU), and as a positive number. Otherwise, reported positive fluxes are directed into the water column and vice versa. Separate BIGO sediment cores were collected by pushing short liners (10 cm in diameter, approximately 20 cm in length) into the 205 sediment within the incubation chambers after BIGO retrieval. Sediment cores were subsampled, and porewater was extracted similarly to MUC cores. The BIGO incubation chambers were also subsampled for SRR measurements, directly inserting three acrylic tubes into each chamber after recovery of the lander. Samples were treated identical to those from MUC cores.

# 2.4 In situ flux O<sub>2</sub> measurements with Deep-sea Rover (DSR) Panta Rhei

In addition to the fluxes measured using the BIGOs, the autonomous Deep-Sea Rover (DSR) Panta Rhei was used to repeatedly measure O<sub>2</sub> uptake in the HI and the CL. The DSR represents a six-wheeled vehicle (weight in air 1200 kg, 80 kg in water, dimensions 3 x 2 x 1.7 m (L, W, H)), which is specifically designed to carry out repeated benthic oxygen flux measurements inside two benthic incubation chambers at the front of the vehicle for prolonged time periods of up to one year.

O<sub>2</sub> was measured using fiber-optic O<sub>2</sub> sensors (Pyroscience, Bremen), three were placed inside each flux chamber, two sensors record the O<sub>2</sub> variability in the ambient bottom water. The volume of the two benthic chambers was either determined automatically by injecting pure water into the benthic chambers after the measurement and simultaneously recording the change of the conductivity (Aanderaa conductivity sensors) or by vertical centimeter scales mounted at the outside of each transparent chamber. From these data, the TOU was determined in same way as for the BIGOs. Additionally, the rover carried three camera systems; two of which were forward looking focusing on the sediment area where flux measurements are conducted by the left and right flux chamber, whereas the third camera was backward looking.

Upon its placement on the seafloor, the following sequence of activities was performed by the rover: i. after placement, it moved a distance of several meters away from its landing site into an undisturbed area, ii. the benthic chambers were flushed, iii. photos taken of the area that will be sampled by the two benthic chambers iv. benthic chambers inserted into the sediment and flushed prior to the start of flux measurement, v. photos taken of both chambers whilst inserted into the sediment (these photos can be used for the volume determination of each chamber), vi. measurement phase, duration was set to 8 hours, the sampling interval of the optodes was set to 5 min. vii. after the measurement phase, pure water was injected to determine the volume of both chambers, and the change of conductivity was monitored for 20 min at an increased sampling rate, viii. the chambers were raised out of the sediment and photos of the sampled area were again taken, ix. the rover advanced 0.7 m to the next measurement area. Apart from step i, this sequence was repeated until the recovery of the rover.

# 2.5 Geochemical analyses of sediments

240

260

Porewater samples were immediately analyzed for TA, dissolved nutrients (TPO<sub>4</sub>³-, NO<sub>5</sub>-, NO<sub>2</sub>-, NH<sub>4</sub>+, and H<sub>4</sub>SiO<sub>4</sub>), Fe²+, and dissolved hydrogen sulfide (H<sub>2</sub>S). TA was measured by titrating 0.5–1 mL of sample with 0.02 N HCl using a color indicator (mixture of methylene blue and methyl red), following the method of Ivanenkov and Lyakhin (1978). The endpoint was identified by the appearance of a stable pink color. During titration, the sample was degassed by continuous nitrogen bubbling to eliminate any CO<sub>2</sub> and H<sub>2</sub>S produced. Standardization was performed with the International Association for the Physical Sciences of the Oceans (IAPSO) seawater solution, achieving an analytical precision error for TA of better than 3%.

Porewater H<sub>2</sub>S, NH<sub>4</sub>+, PO<sub>4</sub><sup>3-</sup>, and H<sub>4</sub>SiO<sub>4</sub> concentrations were determined by standard spectrophotometric methods using a Hitachi U-2001 spectrophotometer (Grasshoff et al., 1999). NO<sub>3</sub><sup>-</sup> and NO<sub>2</sub><sup>-</sup> were analyzed with a Quaatro Autoanalyzer (Seal Analytic), with an error margin below 2%. Dissolved Fe<sup>2+</sup> concentrations were measured by taking 1 mL subsamples within a glove bag, stabilizing immediately with ascorbic acid, and analyzing within 30 minutes following complexation with 20 µl of ferrozine. The analytical error for Fe<sup>2+</sup> measurement was within ±5%. For H<sub>2</sub>S analysis, a porewater aliquot was diluted with oxygen-free artificial seawater, and sulfide was fixed by the immediate addition of zinc acetate gelatine solution.

Untreated filtered samples were stored for later SO<sub>4</sub><sup>2-</sup>, Cl<sup>-</sup>, and Br<sup>-</sup> analysis via ion chromatography at GEOMAR. Additional subsamples were acidified (20 μl of suprapure HNO<sub>3</sub> added to 2 mL sample) for the analysis of major ions (K, Li, B, Mg, Ca, Sr, Mn, Br, and I) and trace elements by inductively coupled plasma optical emission spectroscopy (ICP-OES). Nutrient concentrations in water samples collected from landers were analyzed using the autoanalyzer, with analytical precision and detection limits reported by Haffert et al., (2013) and Sommer et al. (2025).

The water content of sediment cores was determined at by calculating the difference between the wet and dry weights of the samples. Porosity was then calculated from the water content, assuming a particle density of 2.5 g cm<sup>-3</sup> and a seawater density of 1.023 g cm<sup>-3</sup>. After freeze-drying, samples were ground using ball mills. Dry sediment was used for analysis of total carbon, nitrogen (assumed to be particulate organic N, PON) and total sulfur (TS) using a Euro elemental analyzer. POC content was determined after acidifying the sample with HCl (0.25 N) to transform the inorganic carbon to CO<sub>2</sub>. Particulate inorganic carbon, assumed to be calcium carbonate (CaCO<sub>3</sub>), was determined by weight difference between total and organic carbon. The precision and detection limit of the POC analysis was 0.04 and 0.05 dry weight percent (% C), respectively, while that for CaCO<sub>3</sub> was 2 and 0.1 % C.

- The pyrite content of surface sediments (0 1 cm) was estimated by chromium-reducible sulfur following (Canfield et al., 1986). Freeze-dried and ground samples were used. Liberated sulfur was trapped as zinc sulfide and analyzed by photometry (Cline, 1969). The long-term reproducibility and accuracy of the method were monitored against analysis of pure pyrite mixed with quartz sand and an in-house standard (OMZ-2, Peru margin sediment).
- Sulfate reduction rates (SRR) were quantified at GFZ Potsdam, using the cold chromium distillation technique (Kallmeyer et al., 2004). The sample vials were centrifuged and the supernatant carefully removed. A small aliquot of supernatant was kept for quantification of total radioactivity and the rest was discarded. The sediment pellet was quantitatively transferred into a distillation flask by flushing it out of the centrifuge vial with a total of 15 mL N, N-dimethylformamide (DMF), technical grade. To ensure complete mixing of the sediment with the chemicals a magnetic stir bar was added to the reaction flask. The flask was then connected to a constant stream of nitrogen gas (approximately 5-10 bubbles per second) in order to maintain strictly anaerobic conditions during the distillation. After 10 minutes of bubbling the DMF-sediment suspension with N<sub>2</sub> gas, 8 mL of 6 M hydrochloric

acid (HCl) and 15 mL of 1 M chromium (II) chloride solution were added to the flask via a reagent port. The chemicals will convert all reduced sulfur species (TRIS) to H<sub>2</sub>S, which was driven out of solution by the stream of nitrogen gas. The produced gas was then led from the flask through to a first trap filled with 7 mL of a buffered citric acid solution (19.3 g citric acid, 4 g NaOH in 1 L H<sub>2</sub>O, pH 4) to trap any aerosols potentially containing unreacted <sup>35</sup>SO<sub>4</sub><sup>2-</sup> radiotracer but let all H<sub>2</sub>S pass. Finally, the gas was bubbled through 7 mL of 5% (w/v) zinc acetate solution to trap all H<sub>2</sub>S as ZnS. To prevent overflowing of the zinc acetate trap, a few drops of siliconbased antifoam were added. After 2 hours of distillation, the contents of the zinc acetate trap, containing the produced H<sub>2</sub><sup>35</sup>S were quantitatively transferred into a 20 mL plastic scintillation vial and mixed with 8 mL scintillation cocktail for quantification of radioactivity by scintillation counting.

Sulfate reduction rates were calculated according to the following formula:

$$SRR = \frac{so_4 * \varphi * a_{tris} * 1.06 * 10^6}{a_{tot} * t}$$
 Eq. (1)

where SRR is the sulfate reduction rate (pmol cm<sup>-3</sup> d<sup>-1</sup>); SO<sub>4</sub> is the sulfate concentration in the pore water (mmol L<sup>-1</sup>); φ is porosity, set to 0.7; a<sub>tris</sub> is the radioactivity of total reduced inorganic sulfur (cpm); a<sub>tot</sub> is the total radioactivity used (cpm); t is the incubation time (d); 1.06 is a correction factor for isotopic fractionation; and the factor 10<sup>6</sup> converts from μmol L<sup>-1</sup> to pmol L<sup>-1</sup>.

# 2.6 TA and DIC analysis of water samples

- Samples for TA and DIC analysis were taken according to the slightly modified Standard Operation Procedures described by Dickson et al. (2007). The water samples obtained in the glass tubes were transferred into Pyrex test tubes (volume: 10 mL). Subsequently, a small headspace was applied, removing 0.3 mL of the water sample, and the samples were poisoned with 10 µl of HgCl<sub>2</sub>. The test tubes were closed using greased glass stoppers (Apiezon vacuum grease) secured using plastic clamps, and then stored.
- At GEOMAR laboratories, TA (Dickson, 1981) was titrated automatically in an open measuring cell (Metrohm, volume of measuring cell: 1 to 50 mL) according to Dickson et al. (2007). The sample volume was 1 mL. Hydrochloric acid (0.01 M) was added stepwise and the pH value was continuously recorded using an electrode (Metrohm). The TA concentration was calculated using a modified Gran method (Gran, 1952; Humphreys, 2015). The precision and the deviation from the reference standard were 0.2 and 0.02 %, respectively. The CRM seawater standard Dickson batch #188 was used as the reference standard (total inorganic carbon content: 2099.26 μmol kg<sup>-1</sup>; total alkalinity: 2264.96 μmol kg<sup>-1</sup>, https://www.ncei.noaa.gov/access/ocean-carbon-acidification-datasystem /oceans/Dickson CRM/batches.html).
- The concentration of DIC was measured according to Dickson et al. (2007) using an Apollo SciTech analyzer (Model AS-C5) equipped with an infrared carbon dioxide (CO<sub>2</sub>) detector (Trace Gas Analyzer 7815-01, LICOR).

  The sample (0.6 mL) was mixed with 0.7 mL H<sub>3</sub>PO<sub>4</sub> in an extraction chamber where the DIC is completely converted to CO<sub>2</sub> and measured by infrared spectroscopy. A dilution series of a sodium carbonate standard (Na<sub>2</sub>CO<sub>3</sub>, 100 mM) was prepared for calibration, whereby salt water (7 g l<sup>-1</sup> NaCl) was used for the dilution. The CRM standard (batch 188) served as the reference standard. The precision and the deviation from the standard were 0.2 and 0.3 %, respectively.

## 2.7 Diffusive flux calculations

315

325

The diffusive flux of dissolved constituents in porewater between the bottom water and surface sediment was calculated according to Fick's law:

320 
$$J_C = \phi \times D_s \times (dC/dz)$$
 Eq. (2)

where  $J_C$  represents diffusive flux of solute C at the sediment-water interface,  $\phi$  is porosity,  $D_s$  is the diffusion coefficient in sediments, and dC/dz is the concentration gradient at the sediment-water interface. The diffusion coefficient was derived from the diffusion coefficient in seawater ( $D_{sw}$ ) at in situ temperature and salinity using the following equation (Li and Gregory, 1974):

$$D_s = D_{sw}/\theta^2$$
 Eq. (3)

where  $\theta^2$  accounts for sediment tortuosity calculated according to Boudreau (1997):

330

$$\theta^2 = 1 - \ln(\phi)^2$$
 Eq. (4)

The diffusion coefficient for TA was assumed to be equal to that for bicarbonate ion (Dale et al., 2021a). Concentrations of TA, NH<sub>4</sub><sup>+</sup>, and H<sub>4</sub>SiO<sub>4</sub> gradually increased with sediment depth, which allowed the concentration gradient to be calculated by taking the derivative at the sediment-water interface of an exponential function fitted through the concentration data in the upper 4 cm:

$$C(z) = \alpha - (\alpha - C(0)) \times e^{-\gamma z}$$
 Eq. (5)

340

350

C(z) – concentration at depth z

α – asymptotic concentration at 4 cm depth

C(0) – bottom water concentration

 $\gamma$  – exponential coefficient

345 z – sediment depth

The best fit to the data was determined using the FindFit function in Mathematica software. Concentrations of Fe<sup>2+</sup>, NO<sub>3</sub><sup>-</sup>, NO<sub>2</sub><sup>-</sup>, H<sub>2</sub>S and PO<sub>4</sub><sup>3-</sup> were more scattered and not easily represented by Eq. (5), and their diffusive fluxes were not calculated. To assess variability in porewater fluxes across datasets and to facilitate comparison with the BIGO fluxes, we computed the average flux per site and visualized the distribution using box-and-whisker plots. This descriptive approach provides a visual representation of the spread in the data, facilitating comparisons between the HI and CL areas.

## 2.8 POC degradation rate calculations

The rates of particulate organic carbon degradation (RPOC<sub>TOT</sub>) were estimated using a mass balance approach based on the measured fluxes (F) of O<sub>2</sub>, NO<sub>3</sub><sup>-</sup>, and NH<sub>4</sub><sup>+</sup> (Dale et al., 2014):

$$RPOC_{TOT} = \frac{r_{CN}(2 F_{NH4} r_{NO3} - F_{O2} r_{NO3} - F_{NH4} r_{O2} - F_{NO3} r_{O2})}{2 r_{NO3} - r_{O2} + r_{CN} r_{NO3} r_{O2}}$$
Eq. (6)

where r<sub>CN</sub> represents the atomic ratio of carbon-to-nitrogen (C:N) ratio in organic matter undergoing degradation, calculated from the mean down-core POC and PON contents. r<sub>O2</sub> and r<sub>NO3</sub> were 1 and 0.8, respectively, assuming organic matter with an oxidation state of zero.

## 2.9 Statistical analyses

- Statistical analyses were conducted using the R software package. The non-parametric Mann-Whitney U test was employed for each set of data to assess the variability of fluxes between the HI and CL areas. Additionally, this test was also utilized to understand the difference in porewater profiles and variability in the particulate data between HI and CL areas. p-values <0.05 were considered indicative of statistically significant variability. The following notation is used: \*p < 0.05, \*\*p < 0.01, \*\*\*p < 0.001.
- Linear mixed-effects models were used to assess the natural variability of fluxes over the three-week period. For each flux, models were fitted in R using the lme4 and lmerTest packages, with Area as a fixed effect and Date as

a random intercept to account for temporal variability. Models were estimated by maximum likelihood, and temporal effects were assessed using likelihood ratio tests comparing models with and without the Date random effect. Temporal variability was quantified from the Date random-effect variance, with higher values indicating greater temporal variability. *p*-values < 0.05 were considered statistically significant.

#### 3. Results

375

# 3.1 Environmental conditions at Mecklenburger Bight

- Environmental conditions were monitored during the experiment from 18 July to 9 August 2024 using shipboard measurements of wind speed, wind direction, and surface water temperature (Fig. 2). Additionally, bottom water temperature and dissolved oxygen levels were measured during the different deployments of the DSR. Wind speed varied between 4.4 and 13.7 m s<sup>-1</sup>, with the highest gusts from a northwesterly direction. Correspondingly, sea surface temperature (SST) generally ranged between 18 and 20 °C with an increase to 21 °C by 1 August. The bottom water temperature, initially recorded at 9.8 °C, rose to 10.6 °C over the study period. Between 18 July and 2 August, bottom water O<sub>2</sub> levels declined from approximately 100 μmol L<sup>-1</sup> to a minimum of 46 μmol L<sup>-1</sup>. Notable fluctuations in O<sub>2</sub> concentrations were recorded between 31 July and 2 August, which coincided with reduced wind speeds and northerly winds. These variations were likely influenced by wind speed oscillations between 0.5 and 6 m s<sup>-1</sup>, inducing seiches along the sloping seabed, where water masses of different O<sub>2</sub> concentrations flowed past the rover.
- 390 A cyanobacterial bloom appeared in the study area between 3 and 6 August. During this period, SST ranged from 20.1 to 21.4 °C. In contrast, bottom water temperature remained decoupled from diurnal surface temperature fluctuations, gradually increasing from 9.7 to 10.3 °C. Simultaneously, bottom water O<sub>2</sub> concentrations increased from 34 to 94 μmol L<sup>-1</sup>. The variations in bottom water temperature and O<sub>2</sub> levels may be influenced by wind forcing, particularly a shift in wind direction from strong alongshore westerly winds to moderate southeasterly winds.

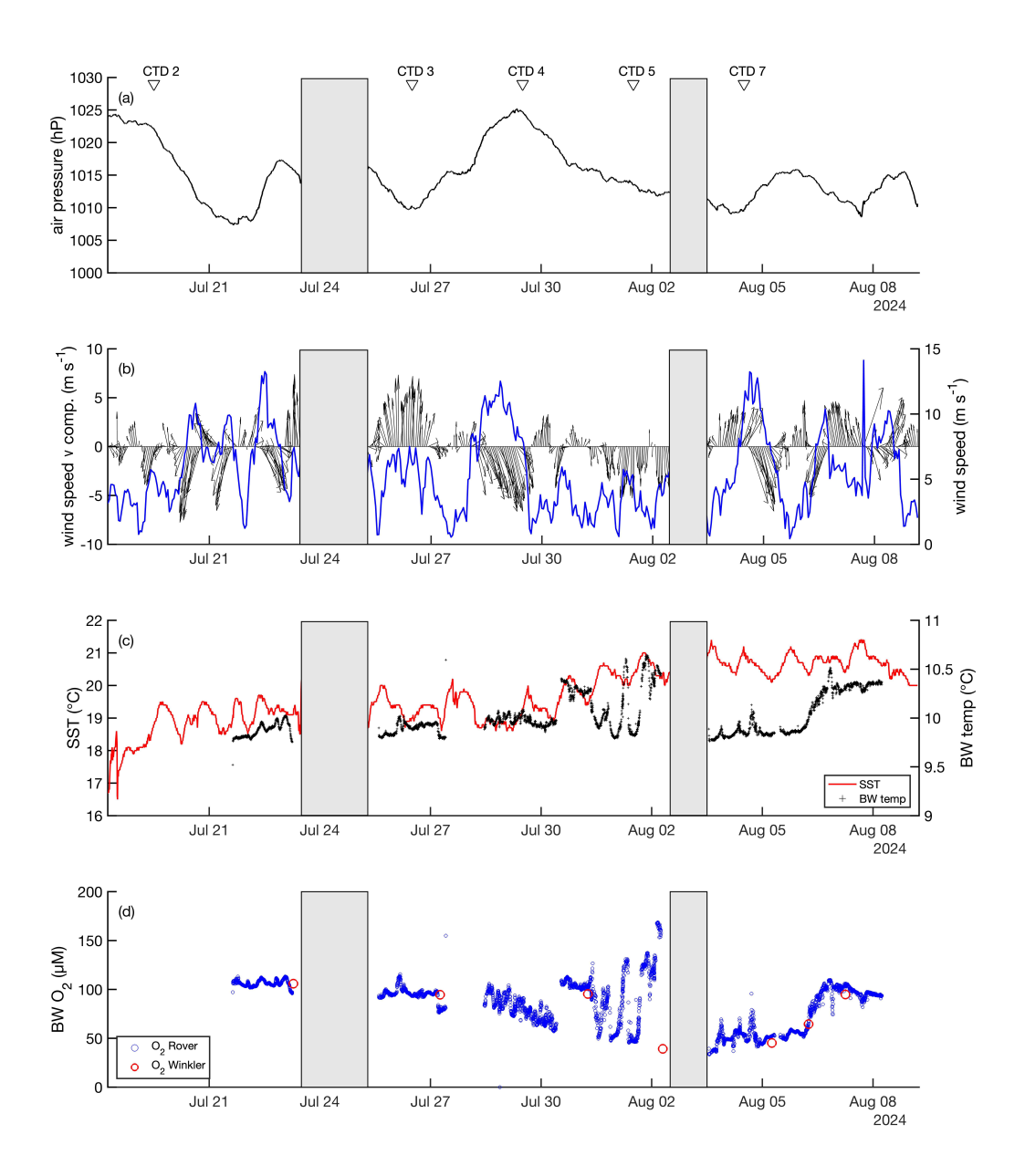


**Figure 2:** Environmental conditions during the time course of the trawling experiment including (a) air pressure, (b) wind speed (blue), wind speed v (north-south) component and direction (black), with arrows indicating orientation, (c) SST (red) and bottom water temperature (black), (d) bottom water dissolved O<sub>2</sub> concentration. Grey bars indicate periods where the ship stayed in harbor. The arrows above the figure denote the CTD deployments.

405

Initially, the thermocline and halocline were located at around 10 m depth and later shifted downwards due to the increase in wind velocity and mixing of the surface layer (Fig. 3). This shift was accompanied by a corresponding deepening of the nutricline. Over time, the chlorophyll-a maxima intensified to almost 15  $\mu$ g L<sup>-1</sup> when the cyanobacterial bloom intensified. In the surface mixed layer, O<sub>2</sub> concentrations were around 300  $\mu$ mol L<sup>-1</sup> and

declined to  $\sim$ 110  $\mu$ mol L<sup>-1</sup> at 4 m above the seafloor. Note that the low O<sub>2</sub> concentrations <100  $\mu$ mol L<sup>-1</sup> recorded by the DSR (Fig. 2) at a distance of  $\sim$ 70 cm above the sediment were not detected by the CTD (maximum depth 5 m above the seafloor).

410

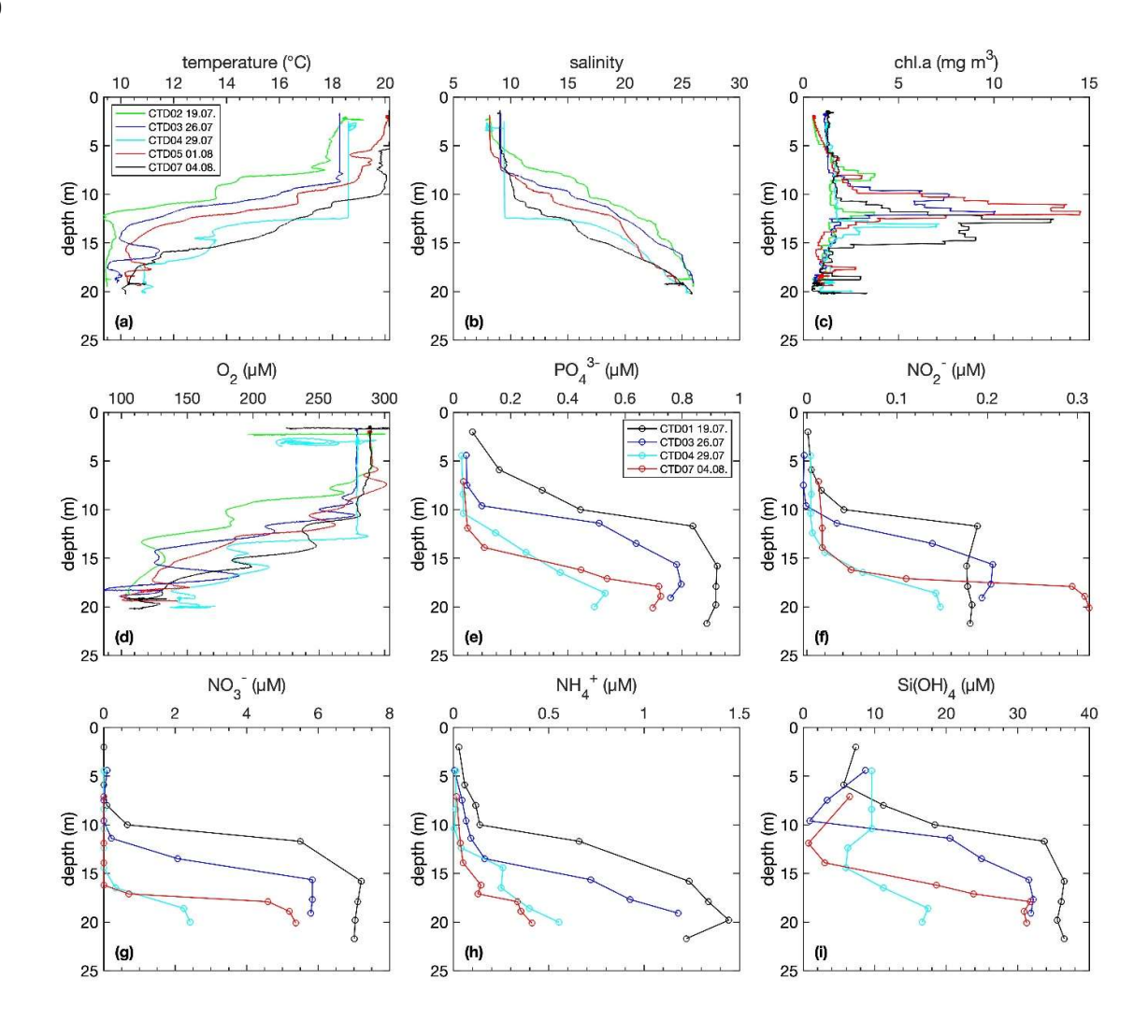


**Figure 3:** Water column distributions of profiles of temperature, salinity, chlorophyll-a, nutrients and oxygen. Note that technical issues were observed with the pumps of CTD03 and CTD04, affecting temperature, salinity, and O<sub>2</sub> in the upper 12 m.

# 3.2 Trawling disturbance

415

420

425

The disturbance caused by the otter boards and footrope, sweeps, chains/, and bridles (compare Figure S1) on the seafloor morphology is distinctly visible in Fig. 4. The images show the undisturbed seabed on the left, characterized by a thin layer of brown phytodetritus. Moving to the right, a sharply defined furrow created by the left trawl board exposed the underlying dark-grey anoxic sediment. A narrow strip of relatively undisturbed sediment is observable adjacent to the furrow, followed by sediment casts on the inward side caused by the otter boards. Further to the right of the sediment casts, another narrow zone of minimally disturbed sediment can be observed. Finally, at the far right of the image, the sediment surface in the net zone has been visibly scraped off by the back strop and sweep line dragging across the seafloor during bottom fishing. A large sediment plume was also observed on the camera system immediately after trawling (not shown).

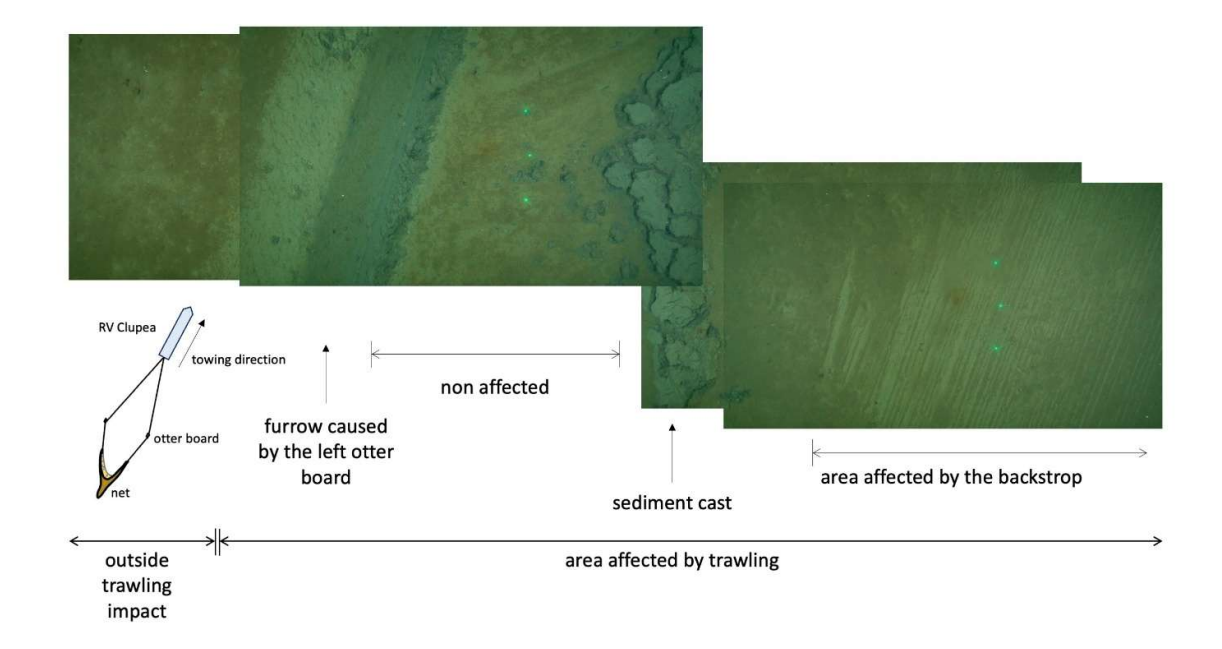


Figure 4: Ocean Floor Observation System (XOFOS) images taken across a trawl mark caused by the left otter board and the net area affected by the back strop and sweep linking the otter boards to the net (compare Fig. S1). The distance between the outer two green laser points is 45 cm. During trawling, the trawl door penetrates the sediment surface, displacing material from the furrow and depositing it towards the inner side. The area in between the otter boards is affected by the back strop, sweep lines, chains, bridles and the footrope and fishing line of the net. This area (referred to as net area) was targeted for sampling in the HI area. Details of the XOFOS deployments are provided in Sommer et al. (2025).

# 3.3 Sediment biogeochemistry and fluxes

430

435

440

445

450

Mean contents of POC, PON, CaCO<sub>3</sub> and TS are presented in Fig. 5 and Table S2, along with organic C:N ratios and porosity. The sediment can be classified as organic-rich and carbonate-poor. POC, PON and CaCO<sub>3</sub> all decreased markedly in the upper 10 cm, and then stabilized at greater depth. TS, in contrast, accumulated to  $\sim 1$  wt. % S. C:N ratios increased from  $\sim 8$  to 9, indicating preferential remineralization of PON relative to POC. All particulate species in the HI area exhibited a slight reduction in the top 2-3 cm compared to the CL area. The surface concentrations of POC, PON, and CaCO<sub>3</sub> were consistently higher at the CL sites (POC:  $3.58 \pm 0.74$  wt.%; PON:  $0.54 \pm 0.11$  wt.%; CaCO<sub>3</sub>:  $5.39 \pm 1.12$  wt.%) compared to the HI sites (POC:  $2.77 \pm 0.78$  wt.%; PON:  $0.41 \pm 0.12$  wt.%; CaCO<sub>3</sub>:  $3.55 \pm 0.48$  wt.%). The reduction of POC in the HI area was close to 1 wt.%. These differences are statistically significant in the upper 1.5 cm, which suggest that surface sediment removal in the net area amounted to the 1-2 cm. This is confirmed by the porosity data, whereby the HI data overlap the CL data when shifted downward by 1.5 cm (Fig. 5f). In the surface sediment layer, the concentrations of TS and C/N ratios showed no significant differences between the CL (TS:  $0.62 \pm 0.13$  wt.%; C/N:  $7.75 \pm 0.26$ ) and HI (TS:  $0.49 \pm 0.17$  wt.%; C/N:  $7.93 \pm 0.38$ ) sites.

Surface pyrite contents in the CL area  $(0.45\pm0.08 \text{ wt.\% FeS}_2)$  were similar to those of HI area  $(0.44\pm0.17 \text{ wt.\% FeS}_2)$ .

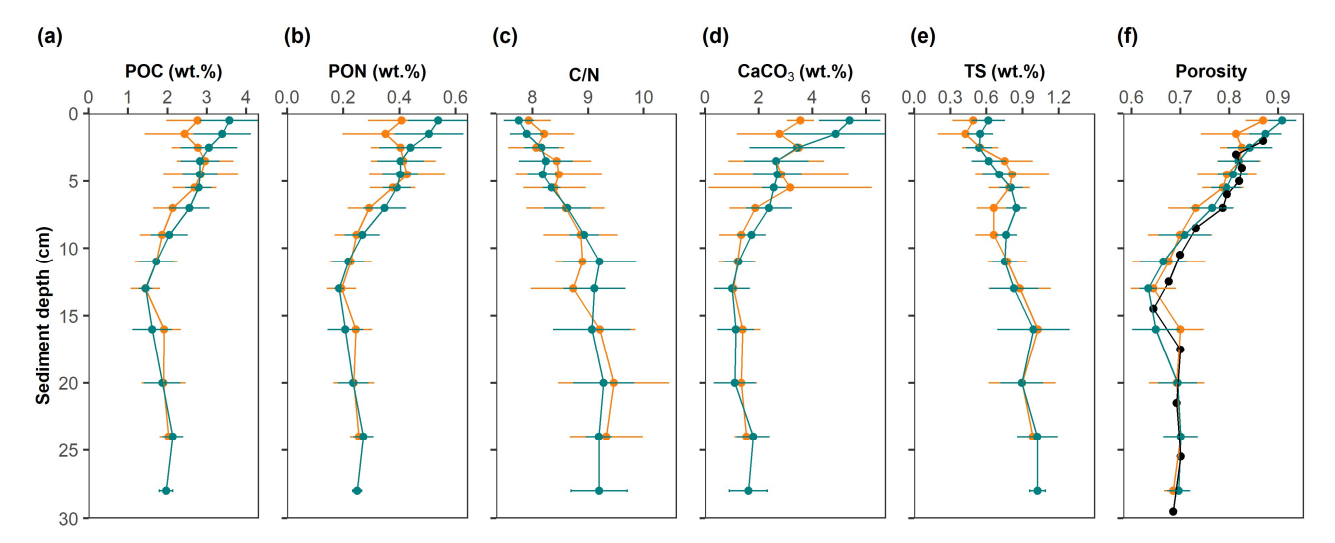
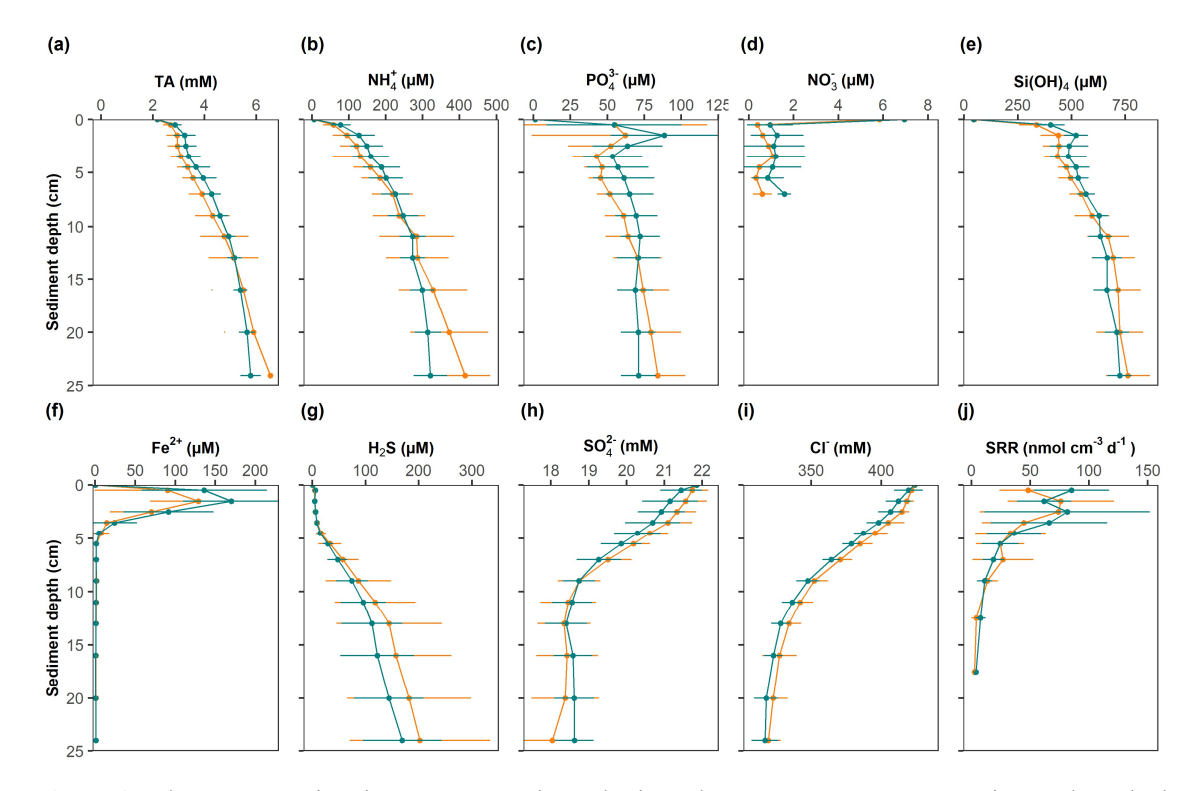


Figure 5: Solid-phase profiles at the study site. Mean values and standard deviations are shown for control sites (green) and high-impact areas (orange). The black points in the porosity profile represent the depth-adjusted values of the HI site assuming surface erosion of 1.5 cm.

Mean solute concentrations measured in MUC samples from CL and HI sites exhibited similar trends (Table S3, Fig. 6). The data have been normalized to chloride concentrations to account for down-core changes in salinity (Fig. 6i). Concentrations of TA,  $NH_4^+$ ,  $PO_4^{3^-}$  and  $H_4SiO_4$  increased with depth due to the remineralization of organic matter. Concurrently,  $SO_4^{2^-}$  decreased by ~4 mM in the upper 10 cm and then showed little further decrease with depth. Concentrations of  $H_2S$  were low in the upper 5 cm where a pronounced  $Fe^{2^+}$  peak was observed.  $H_2S$  then increased to ~200  $\mu$ M at the bottom of the cores.  $NO_3^-$  concentrations were elevated in the top 2 cm and then remained at levels close to the detection limit further down.

465 SRSulfate reduction rates in these organic-rich sediments were elevated very close to the sediment surface and then decreased quasi-exponentially down to ~15 cm. The depth-integrated SRR equaled 4.1±3.1 and 3.1±2.7 mmol S m<sup>-2</sup> d<sup>-1</sup> at the CL and HI sites, respectively. For a simple carbohydrate (i.e. zero C oxidation state), 2 moles of POC are oxidized per mole of SO<sub>4</sub><sup>2</sup>- reduced (e.g., Burdige and Komada, 2011). The SRR thus translates to a POC oxidation rate of 8.3 and 9.5 mmol m<sup>-2</sup> d<sup>-1</sup> at the CL and HI sites.

Concentrations of TA, NH<sub>4</sub><sup>+</sup>, PO<sub>4</sub><sup>3-</sup>, H<sub>4</sub>SiO<sub>4</sub> and Fe<sup>2+</sup> tended to be higher in the upper cm in the CL area compared to the HI area. Conversely, SO<sub>4</sub><sup>2-</sup> tended to be lower, whereas H<sub>2</sub>S showed little difference. However, the variability of solute concentrations between CL and HI were not statistically significant.



**Figure 6:** Solute concentrations in porewaters at the study site and SRR rates. Mean concentrations and standard deviations are shown for control sites (green) and high-impact areas (orange).

Total fluxes (BIGO data) and diffusive fluxes (for TA, NH<sub>4</sub>+, and H<sub>4</sub>SiO<sub>4</sub>) are illustrated in Fig. 7 (and Table \$3\$4). For TA and NH<sub>4</sub>+, the two approaches of flux calculation were consistent with regards to the range and magnitude of the fluxes. H<sub>4</sub>SiO<sub>4</sub> fluxes showed larger differences with lower total fluxes from the BIGO. In general, the sediments were a sink for O<sub>2</sub> and NO<sub>3</sub>- and a source for all other variables. NO<sub>2</sub>- effluxes (not shown) were < 0.05 mmol m<sup>-2</sup> d<sup>-1</sup>. Mean TOU in the control area was 8.9 mmol m<sup>-2</sup> d<sup>-1</sup>, whereas DIC fluxes were much higher (mean 19.5 mmol m<sup>-2</sup> d<sup>-1</sup>), implying a significant contribution of carbonate dissolution to the DIC flux. This is also supported by a high mean TA flux of 12.2 mmol m<sup>-2</sup> d<sup>-1</sup> in the CL area. Following trawling, the fluxes of TOU, TA, DIC, NH<sub>4</sub>+, PO<sub>4</sub><sup>3-</sup>, H<sub>4</sub>SiO<sub>4</sub> all declined compared to the CL area, whereas NO<sub>3</sub>- and NO<sub>2</sub>- fluxes showed little change. Notably, mean total TA and DIC fluxes were much lower in the HI area, falling to 5.4 and 10.2 mmol m<sup>-2</sup> d<sup>-1</sup>, respectively. The lower total fluxes of TA, NH<sub>4</sub>+, PO<sub>4</sub><sup>3-</sup> and H<sub>4</sub>SiO<sub>4</sub> following trawling are further consistent with the lower porewater concentrations. Total fluxes of TA (\*\*p value), DIC (\*p value), NH<sub>4</sub>+ (\*p value), PO<sub>4</sub><sup>3-</sup> (\*p value), and H<sub>4</sub>SiO<sub>4</sub> (\*\*p value) exhibited statistically significant differences between the HI and CL areas. The diffusive fluxes of TA and H<sub>4</sub>SiO<sub>4</sub> were not significant, whereas NH<sub>4</sub>+ (\*p value) showed significant differences between CL and HI areas.

Control area estimates of RPOC<sub>TOT</sub> equaled 9.6 mmol m<sup>-2</sup> d<sup>-1</sup>, and were followed by a statistically significant (\*p value) decrease after trawling to 7.8 mmol m<sup>-2</sup> d<sup>-1</sup> (Fig. 7h). These are very similar to the TOU, which provides confidence in the RPOC<sub>TOT</sub> calculation. They are also similar to the depth-integrated SRR calculated above. Sulfate reduction is thus the major carbon remineralization pathway, as expected for organic-rich coastal sediments (e.g. Jørgensen, 2021; van de Velde et al., 2018).

Over the 16-day observation period in the HI area, the BIGO fluxes exhibited temporal variability, likely reflecting the gradual recovery of environmental conditions post-trawling (Fig. 8). TA and DIC effluxes and TOU apparently did not fully recover to the CL values by the end of the sampling program. The linear mixed-effects model analysis indicated that TOU, TA, and DIC exhibited natural temporal variability (Date random-effect variance > 0). Temporal trends in the fluxes of NH<sub>4</sub><sup>+</sup>, PO<sub>4</sub><sup>3-</sup>, and H<sub>4</sub>SiO<sub>4</sub> were less clear, although there is a tendency for higher

fluxes in the CL area versus the HI area. No significant natural temporal variability was detected for the other parameters (Date random-effect variance  $\sim$  0).

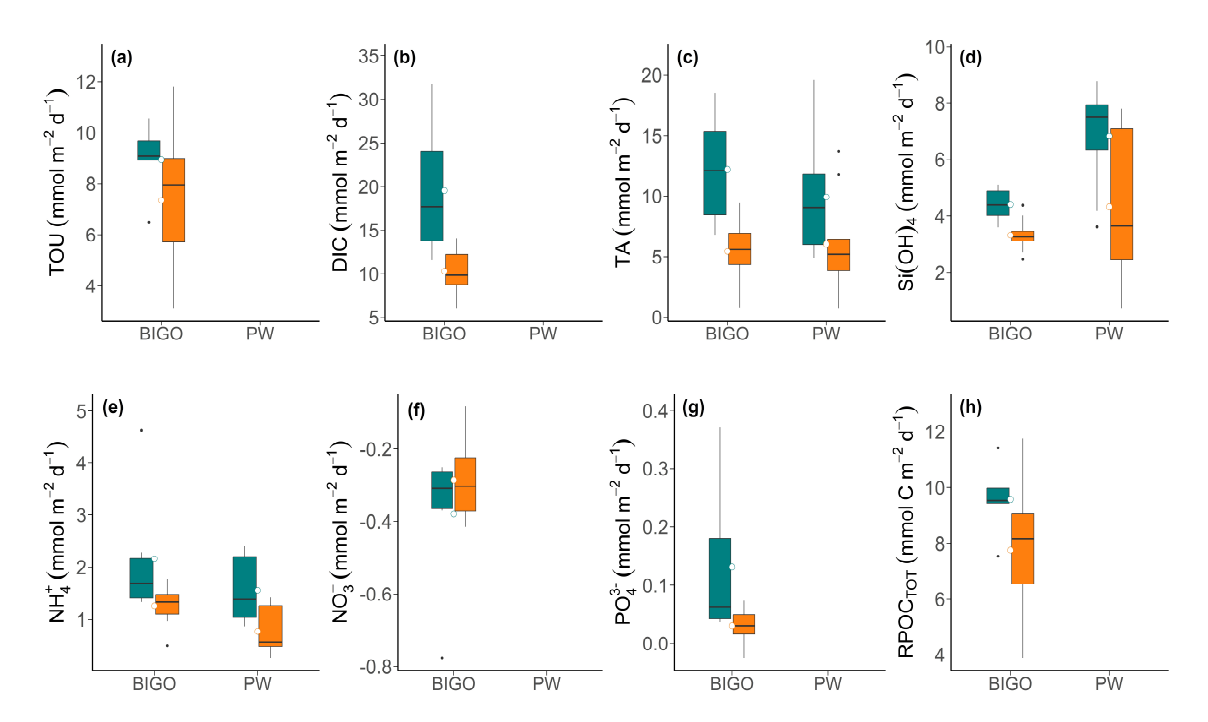


Figure 7: (a-g) Box-whisker plots showing solutes fluxes across the sediment-water interface calculated from lander data (BIGO) and porewater profiles (PW) at the control (green) and high-impact sites (orange). Mean fluxes are shown by the small circles. (h) POC remineralization rates were calculated using Eq. 5.

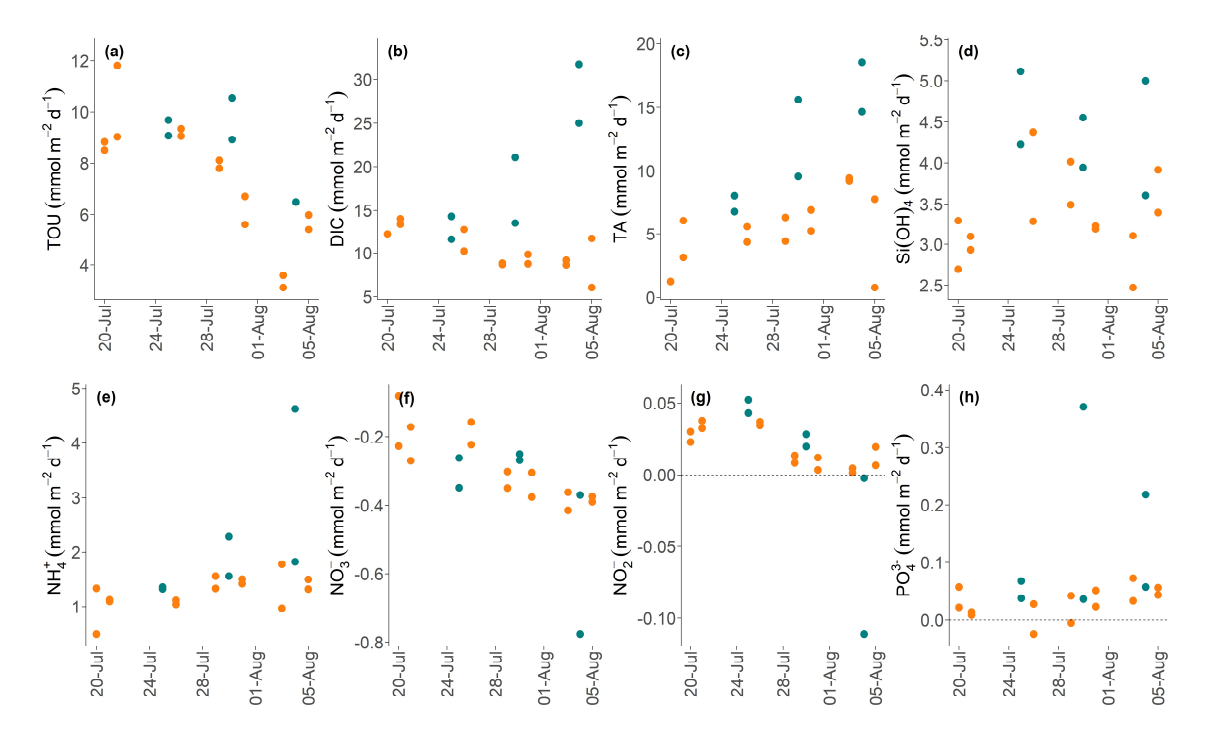


Figure 8: Plots showing the temporal evolution of total fluxes of solutes across the sediment-water interface (in mmol m<sup>-2</sup> d<sup>-1</sup>) over 16 days in control (green) and high-impact (orange) areas determined from the BIGO data. Dashed horizontal lines indicate zero flux.

# 4. Discussion

515

520

525

530

535

# 4.1 Changes in TOU and nutrient fluxes in the net zone

The seafloor photographic images strikingly demonstrate the impact of trawling on sediment morphology (Fig. 4). Sediment was unevenly tossed into the net area by the otter boards, as evident in previous benthic images and model simulations (Bradshaw et al., 2021; Ivanović et al., 2011). In this study, we provide a comprehensive data set on biogeochemical fluxes based on in situ measurements using benthic landers, including DIC and TA fluxes. Focus is on the wide net area, which is far larger than that disturbed by the otter boards (1 - 2 m). Besides, for practical reasons, it was not possible to target the narrow mound and furrows gauged out by the otter boards with our large lander and coring equipment. The trawl marks were sampled by SCUBA divers using push cores, and this data set will be published in a forthcoming manuscript.

An important finding of the study relates to the total fluxes calculated using BIGO data and diffusive fluxes calculated using porewater gradients. The two approaches exhibited slight differences in magnitude for TA and NH<sub>4</sub><sup>+</sup>, whereas total H<sub>4</sub>SiO<sub>4</sub> fluxes were notably lower (Fig. 7). This mismatch could be of some concern since biogenic silica recycling efficiencies are often calculated using porewater concentration gradients (Dale et al., 2021b). Diffusive fluxes derived from concentrations measured in 1-cm intervals fail to capture the porewater gradients just below the sediment surface and do not account for non-diffusive fluxes arising from bioirrigation (Apell et al., 2018). In contrast, the fluxes obtained from benthic chambers integrate all the net sources and sinks across the sediment surface (Tengberg et al., 1995). Since porewater concentrations of H<sub>4</sub>SiO<sub>4</sub> were higher than in the bottom water, bioirrigation would tend to flush out H<sub>4</sub>SiO<sub>4</sub> and augment the total flux. A large sink for H<sub>4</sub>SiO<sub>4</sub> in the upper centimeter could account for the lower BIGO fluxes, although we find this hard to envisage given current knowledge about silica cycling in marine sediments (DeMaster, 2003). The lower benthic chamber fluxes thus suggest that the curve fitting procedure overestimates the H<sub>4</sub>SiO<sub>4</sub> flux at Mecklenburger Bight, but not for TA and NH<sub>4</sub><sup>+</sup>.

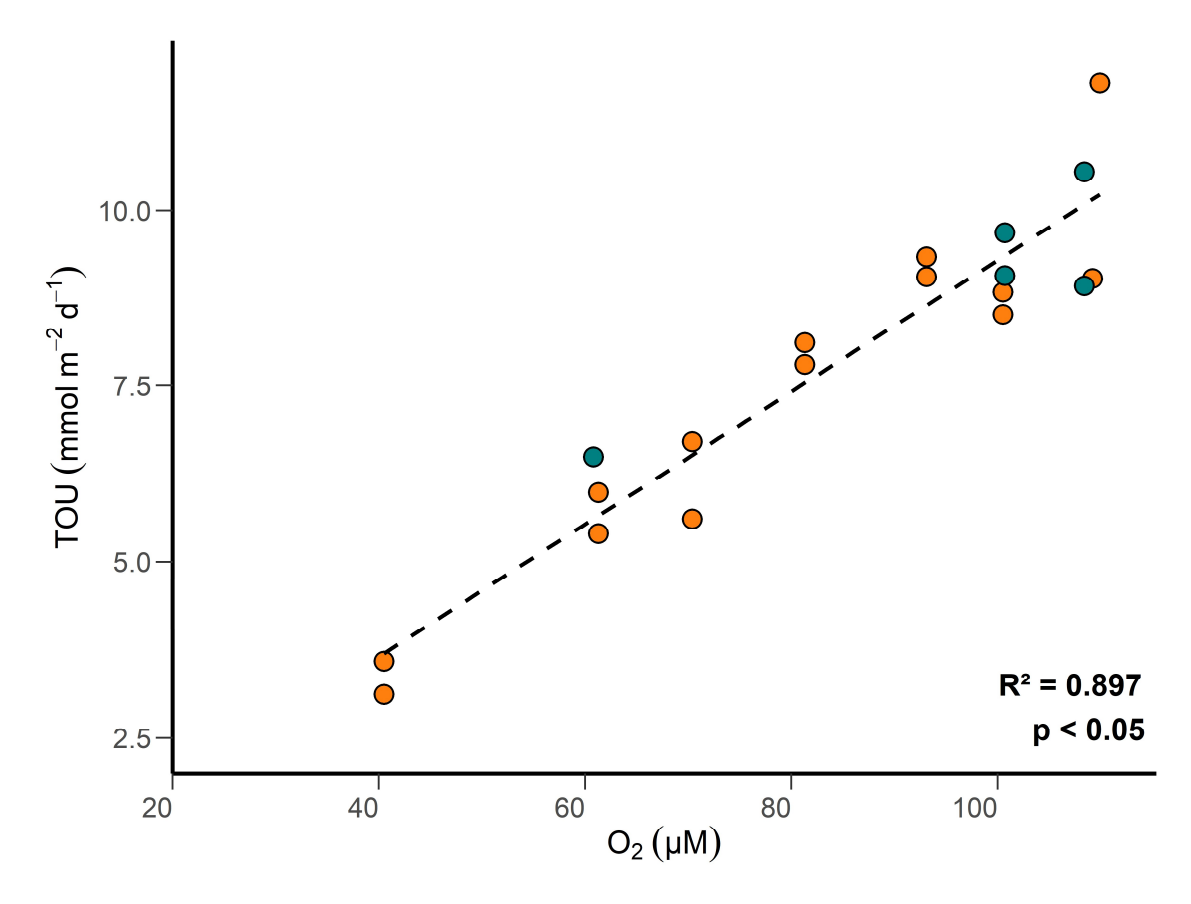


**Figure 9:** TOU versus bottom water oxygen concentration measured by the rover in control (green) and high-impact (orange) areas.

Oxygen concentrations in surface sediments are primarily regulated by the metabolic activities of micro-, meio-, and macrofauna, as well as the oxidation of reduced substances such as NH<sub>4</sub>+, Fe<sup>2+</sup> and H<sub>2</sub>S (Glud, 2008). TOU is further regulated by the content of reactive POC and the bottom water O<sub>2</sub> concentrations. At concentrations < 125 μM, characteristic of our study site, TOU is predicted to correlate positively with bottom water O<sub>2</sub> concentration (Cai and Reimers, 1995). Above 125 μM, the amount of organic carbon in the sediment becomes the critical factor. Our data show this behavior clearly (Fig. 9). The decline in bottom water O<sub>2</sub> concentrations over the study period (Fig. 2) proves to be an important control on TOU. Previous research has reported that trawling lowers O<sub>2</sub> consumption rates in sedimentary ecosystems by effectively stripping away surface sediments and associated microbial and faunal communities and by diminishing the availability of labile reduced substances (Allen and Clarke, 2007; Tiano et al., 2019; Bradshaw et al., 2024). Our findings suggest that trawling has a relatively minor impact on TOU flux in the HI area compared to the role of bottom water O<sub>2</sub> depletion. Similar observations have been reported in previous studies (Goldberg et al., 2014; Trimmer et al., 2005; Warnken et al., 2003), which also found limited effects of trawling on TOU. However, these studies did not explicitly assess the influence of declining bottom-water oxygen concentrations. We ascribe this feature to transport limitation of O<sub>2</sub> across the diffusive boundary layer when O<sub>2</sub> levels fall over time (Bouldin, 1968; Middelburg and Levin, 2009).

The reduction in benthic NH<sub>4</sub><sup>+</sup> fluxes post-trawling contrasts with Morys et al. (2021), who reported an increase immediately afterwards. They attributed this to NH<sub>4</sub><sup>+</sup>-enriched porewater at the newly formed sediment-water interface and the subsequent diffusion of NH<sub>4</sub><sup>+</sup> to the bottom water. Similarly, Duplisea et al. (2001) reported that the NH<sub>4</sub><sup>+</sup> flux from trawled sediment was 45 times higher than the flux from undisturbed sediments. Our findings align more with Bradshaw et al. (2021), who observed a decrease in NH<sub>4</sub><sup>+</sup> flux and argued that it was caused by NH<sub>4</sub><sup>+</sup> depletion following surface sediment removal or from a deceleration of biogeochemical turnover rates. Almroth-Rosell et al. (2012) also found that sediment resuspension resulted in decreased NH<sub>4</sub><sup>+</sup> efflux (~50%) in a benthic chamber investigation, which they ascribed to oxidation of NH<sub>4</sub><sup>+</sup> stimulated by nitrification (Almroth-Rosell et al., 2012). We argue for a simpler explanation for our site, whereby the lower NH<sub>4</sub><sup>+</sup> fluxes were caused

565 by removal of the reactive surface layer associated with the highest rates of ammonification; a finding unambiguously borne out by the reduction in DIC and TA fluxes, as well as by diagenetic modelling (De Borger et al., 2021). The same reasoning applies to the reduction in H<sub>4</sub>SiO<sub>4</sub> fluxes. The dissolution of biogenic silica, mainly diatoms in the Baltic Sea, is the main source of silicate in porewaters (Tréguer and De La Rocha, 2013). Given that dissolution rates are highest at the sediment surface where opal undersaturation is greatest (Rabouille 570 et al., 1997), it logically follows that removal of this layer will immediately diminish the benthic H<sub>4</sub>SiO<sub>4</sub> flux.

Mean fluxes of  $NO_3^-$  into the sediment  $(0.3 - 0.4 \text{ mmol m}^{-2} \text{ d}^{-1})$  were not significantly different between the CL and HI sites, suggesting that denitrification rates in the net area remained stable despite trawling activities if the NO<sub>3</sub><sup>-</sup> flux can be assumed to be a proxy for denitrification. Model results by De Borger et al. (2021) applicable to the net area predicted that increased oxygenation due to bottom trawlingMBCF may double denitrification rates by enhancing NO<sub>3</sub> availability, possibly due to higher rates of coupled nitrification-denitrification. In contrast, intensive fishing activities may reduce NO<sub>3</sub>- concentrations through increased microbial activity, excessive sediment mobilization, and net N loss from sediments (Hale et al., 2017). Ferguson et al., (2020) also reported that benthic trawling altered sediment redox profiles and reduced denitrification rates by 50%, based on N<sub>2</sub> flux data. The similarity of NO<sub>3</sub> fluxes between the CL and HI areas could thus be driven by a combination of lower denitrification rates in combination with NO<sub>3</sub> loss to the water column. This variability of the trawling impact on the direction of the benthic fixed N source/sink, in addition to the variety of methods used, highlights the confounding complications of site-specific environmental factors, such as benthic fauna, nutrient availability and oxygen penetration depth on the N cycle (Sciberras et al., 2016).

Our data nonetheless show that trawling leads to a net decline in the benthic fixed N source to the water column. The exact cause of the N loss (e.g. increased denitrification versus porewater NH<sub>4</sub><sup>+</sup> efflux to the water column) is difficult to constrain and would require detailed laboratory studies to gain further insight. Post-trawling porewater concentrations of PO<sub>4</sub><sup>3</sup> were elevated immediately below the sediment surface (Fig. 6), and it follows that scraping off surface sediment by trawling mixes surface porewater PO<sub>4</sub><sup>3-</sup> into the lower water column, as previous findings have shown (Bradshaw et al., 2021; Duplisea et al., 2001; Sciberras et al., 2016). We currently lack data on bottom water chemistry immediately after trawling to track the missing PO<sub>4</sub>3- after sediment resuspension. Since P cycling in sediments is to a large degree controlled by the redox cycling of Fe (Slomp et al., 1996), it remains to be shown whether the lower PO<sub>4</sub><sup>3</sup>- flux was instead caused by adsorption onto freshly formed iron (oxyhdr)oxides following resuspension (Almroth-Rosell et al., 2012). The observed reduction in porewater Fe<sup>2+</sup> concentrations after trawling could be evidence for this, although presently this is only speculation.

Despite the large number of in situ lander operations over the 16-day experimental period, the recovery time of the sediments with regards to fluxes is difficult to unequivocally reconcile for all chemical components (Fig. 8). DIC, TA and H<sub>4</sub>SiO<sub>4</sub> were consistently higher in the undisturbed control area, whereas for the other nutrients the HI fluxes seemed to converge to the CL fluxes soon after trawling. Yet, the temporal variability of the control fluxes makes it hard to define a robust control baseline, and this is a crucial point that should be noted for all 600 published and planned fieldwork studies on this topic. The temporal decrease in bottom water O<sub>2</sub> is an additional complication since it will affect the rates of carbon cycling and associated redox processes. However, results from long-term (~weeks) ex situ core incubations in the oxygen minimum zone off NW Africa show that benthic fluxes only begin to be altered when dissolved  $\mathrm{O}_2$  falls below  $\sim\!20~\mu\mathrm{M}$  and with a time lag of 1-2 days (Schroller-Lomnitz et al., 2019). Bottom water dissolved O<sub>2</sub> at Mecklenburger Bight was consistently above this threshold (Fig. 2).

# 4.2 Bottom trawling MBCF and organic carbon remineralization

575

580

585

590

595

605

610

615

The organic carbon remineralization rate calculated from our benthic flux measurements (RPOC<sub>TOT</sub>) showed a decline following trawling activities. This reduction is further evident from the in situ DIC and TOU flux measurements. Understanding the impact of trawling on ocean carbon storage is key to predict anthropogenicallyinduced changes to the benthic carbon cycle, yet it remains a subject of considerable debate (Epstein et al., 2022; Zhang et al., 2024). Trawling-induced mechanical disturbance can increase the oxygen exposure of POC buried in sediments, thereby promoting aerobic remineralization and subsequently affecting atmospheric CO<sub>2</sub> uptake (Atwood et al., 2024; Sala et al., 2021). Although oxygen exposure is a major control on organic matter remineralization (Dauwe et al., 2001), other factors are also important. These include the age and composition of organic matter, associated biological communities such as microbes, particle grain size and mineralogy as well as

the local hydrodynamic conditions (Aller et al., 1996; Arndt et al., 2013; Arnosti and Holmer, 2003; Burdige, 2007; Hedges and Keil, 1995).

The surface layer of the sediments holds a high abundance of microbial and macrofaunal communities (Dauwe and Middelburg, 1998; Watling et al., 2001). Our porosity profiles (Fig. 5f) strongly implies that the upper 2 cm might have been scraped away by the ground rope, in agreement with other trawling experiments (Tiano et al., 2019; Bradshaw et al., 2021). The physical disturbance of the surface sediments along with the removal of fauna may decelerate biogeochemical processing and thereby reduce carbon remineralization rates (De Borger et al., 2021; Morys et al., 2021; Pusceddu et al., 2014; Tiano et al., 2019). Fishing experiments conducted in the North Sea reported a decline in benthic metabolic activity immediately after sediment disturbance (Tiano et al., 2019), whereas other model studies suggest little change (Rooze et al., 2024) or even an increase (e.g. van de Velde et al., 2018).

Sediment grain size plays a crucial role in POC remineralization, since fine-grained particles act as preservation nuclei for organic carbon (Hedges and Keil, 1995). A sediment resuspension experiment conducted in the Kiel Bight (Baltic Sea) suggests that grain size controls the difference between remineralization rates under oxic and anoxic settings, with higher rates under oxic conditions for coarser sediments (Kalapurakkal et al., 2025). At Mecklenburger Bight, the sediments are predominantly fine-grained, which should help to protect against carbon remineralization by adsorption onto mineral surfaces. However, although the abundance of fine-grained sediment plume was very prominent, we made no attempt to determine the fate of sediment resuspended in the sediments. Furthermore, Tiano et al. (2019) observed that while reductions in total organic carbon may be subtle, bettom trawlingMBCF disproportionately affects the more reactive fractions of organic carbon. In certain depositional environments, fine-grained suspended sediments may be transported and redeposited in different locations, potentially increasing seabed POC content in downstream areas (Epstein et al., 2022; Palanques et al., 2014). Continuous scraping and ploughing of the surface sediments can also lead to the enrichment of POC due to the upliftment of organic-rich deeper sediments (Palanques et al., 2014). Based on the evidence at hand, we suggest that the reduction in POC remineralization rates shown by our flux measurements can be attributed to the curtailment of biological respiration caused by the removal of the sediment surface.

# 4.3 Impact of benthic alkalinity losses on air-sea CO2 fluxes

620

625

630

635

640

645

650

655

660

665

Literature discussions on the impact of trawling on air-sea CO<sub>2</sub> exchange have focused on the oxidation of resuspended organic carbon as the principle agent of enhanced CO<sub>2</sub> release (Atwood et al., 2024; Hiddink et al., 2023; Sala et al., 2021). Yet, it has recently been shown that pyrite oxidation in the water column induced by sediment resuspension has a far higher potential to induce CO<sub>2</sub> emissions to the atmosphere and a weakening of the carbon shelf pump (Kalapurakkal et al., 2025). This is particularly significant because pyrite formation and burial are major contributors to alkalinity generation and play a crucial role in long-term carbon storage (Hu and Cai, 2011; Reithmaier et al., 2021). A study by van de Velde et al. (2025) further indicated that trawling and dredging reduce natural alkalinity production, thereby weakening the marine carbon sink. Their global estimate indicates that this loss of alkalinity could result in the release of approximately 4.9 Tg CO<sub>2</sub> per year from the ocean to the atmosphere. Our results add to this body of knowledge by showing that trawling also causes a large and immediate reduction in benthic DIC and TA emissions by roughly 50 % (by 9.23 and 6.78 mol m<sup>-2</sup> d<sup>-1</sup>, respectively), which then persists for at least two weeks. The observed reduction in TA and DIC in the present study may be attributed to decreased remineralization of POC in addition to the removal of the undersaturated layer were calcite dissolution is occurring. Once resuspended, it is likely that remineralization of organic carbon to DIC will continue to some extent, although the associated release of alkalinity will be limited to ammonium release. From a benthic perspective, our data demonstrate a pronounced temporal alteration of ecosystem functioning and structure. To the best of our knowledge, these are the first in situ measurements of TA and DIC fluxes in the net area disturbed by trawling.

Data on TA fluxes determined in situ using benthic chambers in the Baltic Sea are rare. Previously, using the BIGOsBIGO landers, TA fluxes of 7-23 mmol m<sup>-2</sup> d<sup>-1</sup> were determined for the Fehmarn Belt and 8-30 mmol m<sup>-2</sup> d<sup>-1</sup> in fine-grained sediments of the Eastern Gotland Basin (Sommer et al., unpublished data). In the Gulf of Gdansk, diffusive carbonate alkalinity fluxes of 1-2 mmol m<sup>-2</sup> d<sup>-1</sup> have been reported (Łukawska-Matuszewska and Dwornik, 2025). High benthic TA release thus appears to be characteristic of muddy sediments in the Baltic Sea, which may partly be caused by benthic carbonate dissolution (Wallmann et al., 2022). In muddy Baltic Sea

sediments, carbonate dissolution is driven by mineral undersaturation in a thin subsurface layer arising from the acidity produced by aerobic respiration pathways (Dale et al., 2024). Carbonate dissolution results in the release of two moles of alkalinity per mole of DIC:

$$CaCO_3 + CO_2 + H_2O \rightarrow 2HCO_3^- + Ca^{2+}$$
 Eq. (7)

An estimate of carbonate dissolution rates (R<sub>CaDiss</sub>, mmol CaCO<sub>3</sub> m<sup>-2</sup> d<sup>-1</sup>) in the CL area can therefore be made as follows (e.g. Burdige, 2006; Hammond et al., 1996):

$$R_{CaDiss} = 0.5 \cdot (J_{TA} + J_{NO3} - J_{NH4} - 4 \times J_{PvB})$$
 Eq. (8)

where J<sub>TA</sub> (12.2 mmol m<sup>-2</sup> d<sup>-1</sup>) is the mean TA flux at the CL sites, J<sub>NO3</sub> is the NO<sub>3</sub><sup>-</sup> influx into the sediment (0.38 mmol m<sup>-2</sup> d<sup>-1</sup>) and J<sub>NH4</sub> is the ammonium efflux (2.2 mmol m<sup>-2</sup> d<sup>-1</sup>). The burial flux of pyrite J<sub>PyB</sub> (as moles of TA) has been calculated to be 0.9 mmol m<sup>-2</sup> d<sup>-1</sup> using the model described below; similar to values from a global model analysis of coastal muds by van de Velde et al. (2025). Inserting the numbers gives R<sub>CaDiss</sub> = 4.7 mmol m<sup>-2</sup> d<sup>-1</sup>, or 9.4 mmol TA m<sup>-2</sup> d<sup>-1</sup>, which demonstrates that carbonate dissolution is a likely candidate for the bulk of the measured TA flux. This number is near-identical to a global model analysis of coastal muds by van de Velde et al. (2025).

Given widespread trawling activities in the region, it is pertinent to question the broader impact of a ramping down of benthic TA and DIC source by bottom fishing on CO<sub>2</sub> exchange with the atmosphere. A coupled benthic-water column model was used to estimate the impact. The model was previously used to examine the impact of sediment resuspension on air-sea CO<sub>2</sub> exchange in the western Baltic Sea (Kalapurakkal et al., 2025). The sediment compartment accounts for the rain rate of POC to the seafloor, degradation of POC coupled to pyrite production, pyrite oxidation caused by shallow trawling (upper 2 cm, i.e., resuspension by net scraping) and pyrite and POC burial, but did not consider carbonate dissolution. Also considered is the enhanced degradation of POC by exposure to oxygen following trawling although, as mentioned, this has only a minor impact on CO<sub>2</sub> fluxes compared to that induced by pyrite oxidation. The corresponding benthic DIC and TA fluxes are fed directly back to the well-mixed water column compartment in a fully coupled manner. In the water column, there is lateral exchange of TA and DIC, and a flux of CO<sub>2</sub> to or from the atmosphere depending on the strength of the benthic TA and DIC emissions.

690

695

700

705

710

715

Initial environmental parameters were set to the study site values (water depth, salinity, temperature, water column DIC and TA concentrations). The molar ratio between pyrite formation and POC oxidation was adjusted to match the local pyrite contents in CL sediment (0.47 wt.%). Following Kalapurakkal et al. (2025), we obtained the trawling frequency (2 yr<sup>-1</sup>) and disturbed areas (38%) from the ICES Vessel Monitoring by Satellite (VMS) database (for calculation see Amoroso et al., 2018). Trawling was assumed to expose the upper 2 cm to oxygen over a five-day period. Benthic DIC fluxes in the original model were exclusively due to POC degradation, whereas TA fluxes were driven by pyrite burial and oxidation. In this study, the model was modified in two ways; (i) to include eonstantbaseline values of carbonate dissolution at the derived rates of 9.4 mmol TA m<sup>-2</sup> d<sup>-1</sup> and 4.57 mmol DIC m<sup>-2</sup> d<sup>-1</sup>, and (ii) during each trawling event, the benthic DIC and TA fluxes were reduced from the baseline values by 9.2 and 6.7 mol8 mmol m<sup>-2</sup> d<sup>-1</sup> in accordance with the flux data in Fig. 7, and for a period of 21 days. With this approach, we consider that carbon degradation and carbonate dissolution were diminished since most of the degradation and dissolution takes place in surface sediments that were partly removed by trawling. A description of the empirical constraints on trawling frequencies and depths can be found in Kalapurakkal et al. (2025). Our updates to the model are described in the Supplement.

The model results show that each trawling episode leads to pronounced losses of TA, as expected from previous results (Kalapurakkal et al., 2025). Sediments transition from a TA source (positive fluxes) to a large TA sink (negative fluxes) during the first trawl due to pyrite oxidation ("Standard run" red curve in Fig. 10a). Note that only a few percent of ambient pyrite pool need to be oxidized per trawl to account for the TA losses (Kalapurakkal et al., 2025). TA fluxes decrease for each subsequent trawling event due to a long-term impoverishment of pyrite

stocks (Kalapurakkal et al., 2025). The water column is a continuous source of CO<sub>2</sub> to the atmosphere at the study site, with large emission peaks consistent with the pulse of acidity produced by oxidation of resuspended pyrite ("Standard run" red curve in Fig. 10b).

In a second execution of the model, DIC and TA fluxes were not reduced by the values of 9.2 and 6.7 mol m<sup>-2</sup> d<sup>-1</sup> that we observed during trawling. A comparison of the results of this exercise ("No directly imposed TA reduction" black curves in Fig. 10) with the standard run shows that the observed reduction in TA and DIC fluxes by trawling has a very minor, almost negligible, impact on TA fluxes and CO<sub>2</sub> emissions. Integrated over the 10 years, the total CO<sub>2</sub> fluxes to the atmosphere in both model scenarios differ by < 1 %.

725

730

735

740

These initial results show that scraping of the surface sediment in the net area by sweep lines, foot ropes and fishing lines hanging between the otter boards has a demonstrable impact on enhancing atmospheric CO2 emissions at the study site. However, this is almost entirely driven by pyrite oxidation, as shown previously for the Kiel Bight (Kalapurakkal et al., 2025). Lower measured surface pyrite contents in the HI versus CL areas tentatively fit with this finding. Changes in benthic DIC and alkalinity fluxes observed during trawling are related to the declined in POC degradation and carbonate dissolution caused by the removal of reactive surface sediments. These coupled processes have only a small net effect on atmospheric CO<sub>2</sub> since carbon degradation promotes CO<sub>2</sub> release whereas carbonate dissolution induces CO<sub>2</sub> uptake from the atmosphere. The observed decrease in benthic alkalinity fluxes by net scraping provides a very small additional weakening of the shelf carbon pump. Consequently, whilst the physical destruction of the sediment surface and enhanced pyrite oxidation are real causes for environmental concern, the additional and immediate reduction of the background alkalinity flux due to the physical removal of the surface sediment appears to be unimportant for the water column carbonate system. Yet, important Important open questions remain for further investigation, including ultimate physicobiogeochemical reasons for the decline in TA and DIC fluxes observed after the trawling, the impact on aerobic versus anaerobic POC degradation, and a deeper understanding on the exact fate of resuspended sediment, including reduced iron phases.

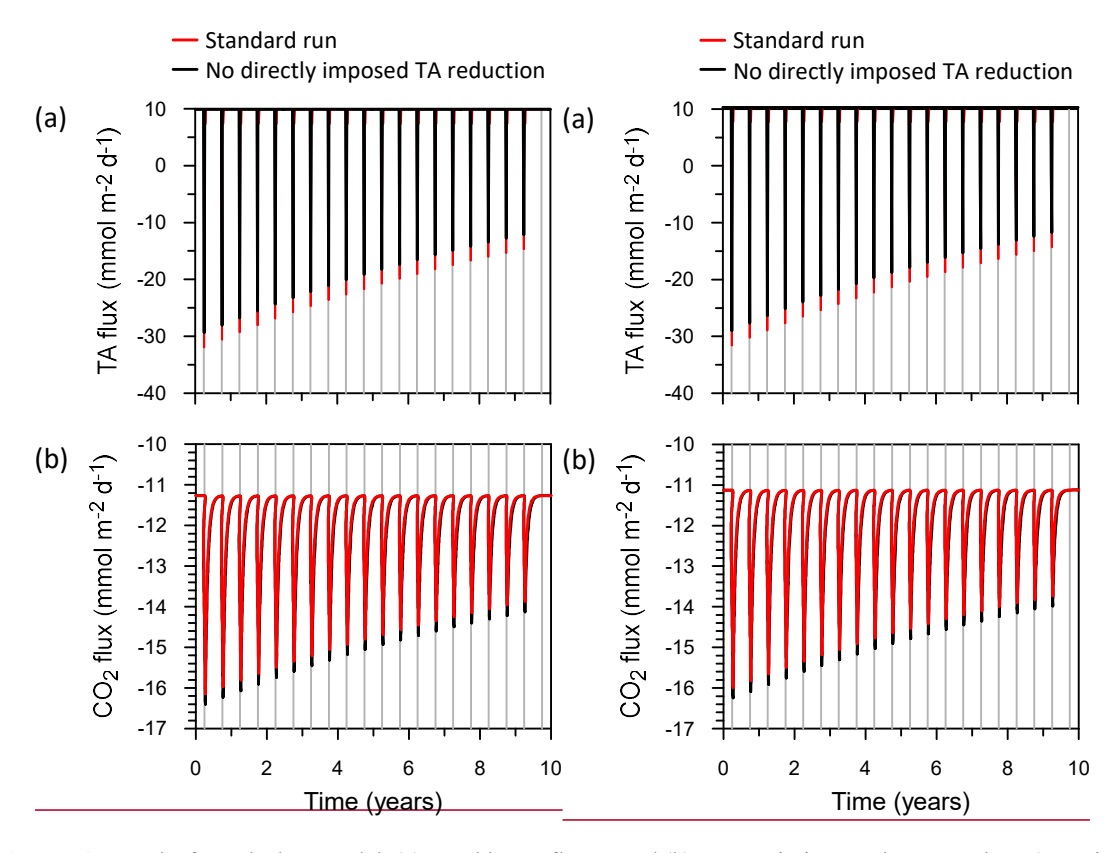


**Figure 10:** Results from the box model. (a) Benthic TA fluxes, and (b) CO<sub>2</sub> emissions to the atmosphere (negative values). Positive TA fluxes represent benthic emissions and vice versa. The red curves show the standard model

run using the observed decrease in TA and DIC fluxes following trawling, and the black curves show the fluxes without these decreases. The vertical grey lines indicate annual trawling events. Note that the red and black curves are mostly superimposed. DIC fluxes are qualitatively similar to TA fluxes (not shown).

#### 5. Conclusions

This field study demonstrates that bottom trawlingMBCF has a profound and lasting impact on benthic remineralization processes. Seafloor imaging vividly illustrates the significant disruption to seafloor morphology, resulting in the resuspension of a sediment plume. Trawling is shown to cause substantial reductions in the fluxes of DIC, TA and nutrients in the net area, which do not fully recover to baseline levels by the end of the 16-day sampling period. The displacement of surface-active sediments directly impedes overall benthic biogeochemical processes, leading to diminished benthic fluxes and a marked reduction in the POC remineralization. Our data underscore that a reduction in biological respiration following the removal of the sediment surface is a key driver of the lower DIC and TA fluxes. A coupled benthic-water column model provides insight into the broader implications of benthic TA losses for CO<sub>2</sub> exchange. Model results suggest that while trawling-induced reductions in TA and DIC fluxes influence carbon cycling, their impact on atmospheric CO<sub>2</sub> sequestration remains minor compared to trawling-induced pyrite oxidation.

To fully understand the long-term consequences of bottom trawlingMBCF, further research should investigate the fate of resuspended sediments, particularly their mineralogical composition and biogeochemical reactivity. However, the temporal and spatial variability of the fluxes within the relatively small control area complicates the characterization of an undisturbed baseline; a caveat that is widely relevant for field studies. Future site-specific studies must also consider local oceanographic conditions and high-trawling-intensity areas to comprehensively assess the cumulative effects of trawling on benthic ecosystems. Such research is critical for informing sustainable fisheries management and mitigating human-induced disturbances in marine environments.

## Acknowledgements

765

785

This work received funding awarded to SS and AD by the German Federal Ministry of Education and Research (BMBF), Grant No. 03F0937F, Project MGF-Ostee, DAM pilot mission: Exclusion of mobile bottom-contact fishing in marine protected areas of the German EEZ of the North Sea and Baltic Sea (MGF North Sea and MGF Baltic Sea). We thank Bettina Domeyer, Regina Surberg, Anke Bleyer, Alexandra Subic, and Frauke Langenberg for assistance during the collection and analysis of sediment samples, and Matthias Türk and Asmus Petersen, and
 Alexandra Subic for gear preparation and deployments. We are also grateful to Gabriel Nolte, Jens Greinert and Martin Pieper for assistance with the XOFOS. The captain and crew of RV Alkor are warmly thanked for their professional and easy-going work environment on board. We thank Daniel Oesterwind for his help with the reviewers' comments on the otter trawl specifications. We greatly appreciate the insights and constructive comments provided by Sebastiaan van de Velde and Sarah Paradis. And finally, to Jack Middelburg for editorial handling of our manuscript.

**Competing interests:** The authors declare that they have no conflict of interest.

**Author Contributions:** S.S. and A.W.D. were responsible for planning and executing the study, as well as funding acquisition. S.S. conducted the BIGO and XOFOS deployments. P. L., H.T.K., and A.W.D. were involved in sediment sampling and analysis. A.W.D. conducted the modeling work. J.K. and S.B. carried out the sulfate reduction measurements, while F.S. performed the pyrite measurements. P. L., A.W.D., and S.S. prepared the manuscript with contributions from all authors.

## References

Allen, J. and Clarke, K.: Effects of demersal trawling on ecosystem functioning in the North Sea: a modelling study, Mar. Ecol. Prog. Ser., 336, 63–75, https://doi.org/10.3354/meps336063, 2007.

- Aller, R. C., Blair, N. E., Xia, Q., and Rude, P. D.: Remineralization rates, recycling, and storage of carbon in Amazon shelf sediments, Cont. Shelf Res., 16, 753–786, https://doi.org/10.1016/0278-4343(95)00046-1, 1996.
- Almroth-Rosell, E., Tengberg, A., Andersson, S., Apler, A., and Hall, P. O. J.: Effects of simulated natural and massive resuspension on benthic oxygen, nutrient and dissolved inorganic carbon fluxes in Loch Creran,

  Scotland, J. Sea Res., 72, 38–48, https://doi.org/10.1016/j.seares.2012.04.012, 2012.
  - Amoroso, R. O., Pitcher, C. R., Rijnsdorp, A. D., McConnaughey, R. A., Parma, A. M., Suuronen, P., Eigaard, O. R., Bastardie, F., Hintzen, N. T., Althaus, F., Baird, S. J., Black, J., Buhl-Mortensen, L., Campbell, A. B., Catarino, R., Collie, J., Cowan, J. H., Durholtz, D., Engstrom, N., Fairweather, T. P., Fock, H. O., Ford, R., Gálvez, P. A., Gerritsen, H., Góngora, M. E., González, J. A., Hiddink, J. G., Hughes, K. M., Intelmann, S. S.,
- Jenkins, C., Jonsson, P., Kainge, P., Kangas, M., Kathena, J. N., Kavadas, S., Leslie, R. W., Lewis, S. G.,
  Lundy, M., Makin, D., Martin, J., Mazor, T., Gonzalez-Mirelis, G., Newman, S. J., Papadopoulou, N., Posen, P.
  E., Rochester, W., Russo, T., Sala, A., Semmens, J. M., Silva, C., Tsolos, A., Vanelslander, B., Wakefield, C.
  B., Wood, B. A., Hilborn, R., Kaiser, M. J., and Jennings, S.: Bottom trawl fishing footprints on the world's continental shelves, Proc. Natl. Acad. Sci., 115, https://doi.org/10.1073/pnas.1802379115, 2018.
- Apell, J. N., Shull, D. H., Hoyt, A. M., and Gschwend, P. M.: Investigating the Effect of Bioirrigation on In Situ Porewater Concentrations and Fluxes of Polychlorinated Biphenyls Using Passive Samplers, Environ. Sci. Technol., 52, 4565–4573, https://doi.org/10.1021/acs.est.7b05809, 2018.
- Arndt, S., Jørgensen, B. B., LaRowe, D. E., Middelburg, J. J., Pancost, R. D., and Regnier, P.: Quantifying the degradation of organic matter in marine sediments: A review and synthesis, Earth-Sci. Rev., 123, 53–86, https://doi.org/10.1016/j.earscirev.2013.02.008, 2013.
  - Arnosti, C. and Holmer, M.: Carbon cycling in a continental margin sediment: contrasts between organic matter characteristics and remineralization rates and pathways, Estuar. Coast. Shelf Sci., 58, 197–208, https://doi.org/10.1016/S0272-7714(03)00077-5, 2003.
- Atwood, T. B., Romanou, A., DeVries, T., Lerner, P. E., Mayorga, J. S., Bradley, D., Cabral, R. B., Schmidt, G. A., and Sala, E.: Atmospheric CO2 emissions and ocean acidification from bottom-trawling, Front. Mar. Sci., 10, 1125137, https://doi.org/10.3389/fmars.2023.1125137, 2024.
  - Bergman, M.: Mortality in megafaunal benthic populations caused by trawl fisheries on the Dutch continental shelf in the North Sea in 1994, ICES J. Mar. Sci., 57, 1321–1331, https://doi.org/10.1006/jmsc.2000.0917, 2000.
- Bergman, M. J. N. and Meesters, E. H.: First indications for reduced mortality of non-target invertebrate benthic megafauna after pulse beam trawling, ICES J. Mar. Sci., 77, 846–857, https://doi.org/10.1093/icesjms/fsz250, 2020.
  - Boudreau, B. P.: Diagenetic models and their implementation, Springer Berlin, 1997.
  - Bouldin, D. R.: Models for Describing the Diffusion of Oxygen and Other Mobile Constituents Across the Mud-Water Interface, J. Ecol., 56, 77, https://doi.org/10.2307/2258068, 1968.
- 825 Bradshaw, C., Jakobsson, M., Brüchert, V., Bonaglia, S., Mörth, C.-M., Muchowski, J., Stranne, C., and Sköld, M.: Physical Disturbance by Bottom Trawling Suspends Particulate Matter and Alters Biogeochemical Processes on and Near the Seafloor, Front. Mar. Sci., 8, 683331, https://doi.org/10.3389/fmars.2021.683331, 2021.
- Bradshaw, C., Iburg, S., Morys, C., Sköld, M., Pusceddu, A., Ennas, C., Jonsson, P., and Nascimento, F. J. A.:

  Effects of bottom trawling and environmental factors on benthic bacteria, meiofauna and macrofauna communities and benthic ecosystem processes, Sci. Total Environ., 921, 171076, https://doi.org/10.1016/j.scitotenv.2024.171076, 2024.
  - Brenner, H., Braeckman, U., Le Guitton, M., and Meysman, F. J. R.: The impact of sedimentary alkalinity release on the water column  $CO_2$  system in the North Sea, Biogeosciences, 13, 841–863,
- 835 https://doi.org/10.5194/bg-13-841-2016, 2016.

- Bruns, I., Bartholomä, A., Menjua, F., and Kopf, A.: Physical impact of bottom trawling on seafloor sediments in the German North Sea, Front. Earth Sci., 11, 1233163, https://doi.org/10.3389/feart.2023.1233163, 2023.
- Bunke, D., Leipe, T., Moros, M., Morys, C., Tauber, F., Virtasalo, J. J., Forster, S., and Arz, H. W.: Natural and Anthropogenic Sediment Mixing Processes in the South-Western Baltic Sea, Front. Mar. Sci., 6, 677, https://doi.org/10.3389/fmars.2019.00677, 2019.
  - Burdige, D. J.: Geochemistry of marine sediments, Princeton University Press, 2006.
  - Burdige, D. J.: Preservation of Organic Matter in Marine Sediments: Controls, Mechanisms, and an Imbalance in Sediment Organic Carbon Budgets?, Chem. Rev., 107, 467–485, https://doi.org/10.1021/cr050347q, 2007.
- Burdige, D. J. and Komada, T.: Anaerobic oxidation of methane and the stoichiometry of remineralization processes in continental margin sediments, Limnol. Oceanogr., 56, 1781–1796, https://doi.org/10.4319/lo.2011.56.5.1781, 2011.
  - Burt, W. J., Thomas, H., Hagens, M., Pätsch, J., Clargo, N. M., Salt, L. A., Winde, V., and Böttcher, M. E.: Carbon sources in the North Sea evaluated by means of radium and stable carbon isotope tracers: Tracing Carbon with Ra and  $\delta^{13}$  C<sub>DIC</sub>, Limnol. Oceanogr., 61, 666–683, https://doi.org/10.1002/lno.10243, 2016.
- Cai, W.-J. and Reimers, C. E.: Benthic oxygen flux, bottom water oxygen concentration and core top organic carbon content in the deep northeast Pacific Ocean, Deep Sea Res. Part Oceanogr. Res. Pap., 42, 1681–1699, https://doi.org/10.1016/0967-0637(95)00073-F, 1995.
  - Canfield, D. E., Raiswell, R., Westrich, J. T., Reaves, C. M., and Berner, R. A.: The use of chromium reduction in the analysis of reduced inorganic sulfur in sediments and shales, Chem. Geol., 54, 149–155, 1986.
- 855 Cline, J. D.: Spectrophotometric determination of hydrogen sulfide in natural waters 1, Limnol. Oceanogr., 14, 454–458, 1969.
  - Corell, H., Bradshaw, C., and Sköld, M.: Sediment suspended by bottom trawling can reduce reproductive success in a broadcast spawning fish, Estuar. Coast. Shelf Sci., 282, 108232, https://doi.org/10.1016/j.ecss.2023.108232, 2023.
- Dale, A. W., Sommer, S., Ryabenko, E., Noffke, A., Bohlen, L., Wallmann, K., Stolpovsky, K., Greinert, J., and Pfannkuche, O.: Benthic nitrogen fluxes and fractionation of nitrate in the Mauritanian oxygen minimum zone (Eastern Tropical North Atlantic), Geochim. Cosmochim. Acta, 134, 234–256, https://doi.org/10.1016/j.gca.2014.02.026, 2014.
- Dale, A. W., Sommer, S., Lichtschlag, A., Koopmans, D., Haeckel, M., Kossel, E., Deusner, C., Linke, P., Scholten, J., Wallmann, K., Van Erk, M. R., Gros, J., Scholz, F., and Schmidt, M.: Defining a biogeochemical baseline for sediments at Carbon Capture and Storage (CCS) sites: An example from the North Sea (Goldeneye), Int. J. Greenh. Gas Control, 106, 103265, https://doi.org/10.1016/j.ijggc.2021.103265, 2021a.
- Dale, A. W., Paul, K. M., Clemens, D., Scholz, F., Schroller-Lomnitz, U., Wallmann, K., Geilert, S., Hensen, C., Plass, A., Liebetrau, V., Grasse, P., and Sommer, S.: Recycling and Burial of Biogenic Silica in an Open
   Margin Oxygen Minimum Zone, Glob. Biogeochem. Cycles, 35, e2020GB006583, https://doi.org/10.1029/2020GB006583, 2021b.
  - Dale, A. W., Geilert, S., Diercks, I., Fuhr, M., Perner, M., Scholz, F., and Wallmann, K.: Seafloor alkalinity enhancement as a carbon dioxide removal strategy in the Baltic Sea, Commun. Earth Environ., 5, 452, https://doi.org/10.1038/s43247-024-01569-3, 2024.
- Dauwe, B. and Middelburg, J. J.: Amino acids and hexosamines as indicators of organic matter degradation state inNorth Sea sediments, Limnol. Oceanogr., 43, 782–798, https://doi.org/10.4319/lo.1998.43.5.0782, 1998.
  - Dauwe, B., Middelburg, J., and Herman, P.: Effect of oxygen on the degradability of organic matter in subtidal and intertidal sediments of the North Sea area, Mar. Ecol. Prog. Ser., 215, 13–22, https://doi.org/10.3354/meps215013, 2001.

- Borger, E., Tiano, J., Braeckman, U., Rijnsdorp, A. D., and Soetaert, K.: Impact of bottom trawling on sediment biogeochemistry: a modelling approach, Biogeosciences, 18, 2539–2557, https://doi.org/10.5194/bg-18-2539-2021, 2021.
  - DeMaster, D.: The diagenesis of biogenic silica: chemical transformations occurring in the water column, seabed, and crust, Treatise Geochem., 7, 407, https://doi.org/10.1016/B0-08-043751-6/07095-X, 2003.
- Depestele, J., Degrendele, K., Esmaeili, M., Ivanović, A., Kröger, S., O'Neill, F. G., Parker, R., Polet, H., Roche, M., Teal, L. R., Vanelslander, B., and Rijnsdorp, A. D.: Comparison of mechanical disturbance in soft sediments due to tickler-chain SumWing trawl vs. electro-fitted PulseWing trawl, ICES J. Mar. Sci., 76, 312–329, https://doi.org/10.1093/icesjms/fsy124, 2019.
- Díaz-Mendoza, G. A., Krämer, K., Von Rönn, G. A., Heinrich, C., Schwarzer, K., Reimers, H.-C., and Winter, C.: Hotspots of human impact on the seafloor in the Southwestern Baltic Sea, Cont. Shelf Res., 285, 105362, https://doi.org/10.1016/j.csr.2024.105362, 2025.
  - Dickson, A. G.: An exact definition of total alkalinity and a procedure for the estimation of alkalinity and total inorganic carbon from titration data, Deep Sea Res. Part Oceanogr. Res. Pap., 28, 609–623, https://doi.org/10.1016/0198-0149(81)90121-7, 1981.
- Dickson, A. G., Sabine, C. L., Christian, J. R., Bargeron, C. P., and North Pacific Marine Science Organization (Eds.): Guide to best practices for ocean CO2 measurements, North Pacific Marine Science Organization, Sidney, BC, 1 pp., 2007.
- Duplisea, D. E., Jennings, S., Malcolm, S. J., Parker, R., and Sivyer, D. B.: Modelling potential impacts of bottom trawl fisheries on soft sediment biogeochemistry in the North Sea†, Geochem. Trans., 2, 112, https://doi.org/10.1186/1467-4866-2-112, 2001.
  - Epstein, G., Middelburg, J. J., Hawkins, J. P., Norris, C. R., and Roberts, C. M.: The impact of mobile demersal fishing on carbon storage in seabed sediments, Glob. Change Biol., 28, 2875–2894, https://doi.org/10.1111/gcb.16105, 2022.
- Ferguson, A. J. P., Oakes, J., and Eyre, B. D.: Bottom trawling reduces benthic denitrification and has the potential to influence the global nitrogen cycle, Limnol. Oceanogr. Lett., 5, 237–245, https://doi.org/10.1002/lol2.10150, 2020.
  - Glud, R. N.: Oxygen dynamics of marine sediments, Mar. Biol. Res., 4, 243–289, https://doi.org/10.1080/17451000801888726, 2008.
- Goldberg, R., Rose, J. M., Mercaldo-Allen, R., Meseck, S. L., Clark, P., Kuropat, C., and Pereira, J. J.: Effects of hydraulic dredging on the benthic ecology and sediment chemistry on a cultivated bed of the Northern quahog, Mercenaria mercenaria, Aquaculture, 428–429, 150–157, https://doi.org/10.1016/j.aquaculture.2014.03.012, 2014.
  - Gran, G.: Determination of the Equivalence Point in Potentiometric Titrations. Part 11, Analyst, 77, 661--671, 1952.
- 915 Grasshoff, K., Kremling, K., and Ehrhardt, M.: Methods of seawater analysis, John Wiley & Sons, 1999.
  - Haffert, L., Haeckel, M., Liebetrau, V., Berndt, C., Hensen, C., Nuzzo, M., Reitz, A., Scholz, F., Schönfeld, J., Perez-Garcia, C., and Weise, S. M.: Fluid evolution and authigenic mineral paragenesis related to salt diapirism The Mercator mud volcano in the Gulf of Cadiz, Geochim. Cosmochim. Acta, 106, 261–286, https://doi.org/10.1016/j.gca.2012.12.016, 2013.
- 920 Hale, R., Godbold, J. A., Sciberras, M., Dwight, J., Wood, C., Hiddink, J. G., and Solan, M.: Mediation of macronutrients and carbon by post-disturbance shelf sea sediment communities, Biogeochemistry, 135, 121– 133, https://doi.org/10.1007/s10533-017-0350-9, 2017.

- Hammond, D., McManus, J., Berelson, W., Kilgore, T., and Pope, R.: Early diagenesis of organic material in equatorial Pacific sediments: stoichiometry and kinetics, Deep Sea Res. Part II Top. Stud. Oceanogr., 43, 1365–925 1412, 1996.
  - Hedges, J. I. and Keil, R. G.: Sedimentary organic matter preservation: an assessment and speculative synthesis, Mar. Chem., 49, 81–115, 1995.
  - HELCOM: State of the Baltic Sea--Second HELCOM holistic assessment 2011--2016, in: Baltic Sea Environment Proceedings, vol. 155, HELCOM, 2018.
- 930 Hiddink, J. G., Jennings, S., and Kaiser, M. J.: Indicators of the Ecological Impact of Bottom-Trawl Disturbance on Seabed Communities, Ecosystems, 9, 1190–1199, https://doi.org/10.1007/s10021-005-0164-9, 2006.
  - Hiddink, J. G., van de Velde, S. J., McConnaughey, R. A., De Borger, E., Tiano, J., Kaiser, M. J., Sweetman, A. K., and Sciberras, M.: Quantifying the carbon benefits of ending bottom trawling, Nature, 617, E1–E2, https://doi.org/10.1038/s41586-023-06014-7, 2023.
- Hu, X. and Cai, W.-J.: An assessment of ocean margin anaerobic processes on oceanic alkalinity budget, Glob. Biogeochem. Cycles, 25, n/a-n/a, https://doi.org/10.1029/2010GB003859, 2011.
  - Humphreys, M. P.: Measurements and Concepts in Marine Carbonate Chemistry, University of Southampton, 2015.
- ICES: Manual for the Baltic International Trawl Surveys (BITS), https://doi.org/10.17895/ICES.PUB.2883, 2017.
  - Ivanović, A., Neilson, R. D., and O'Neill, F. G.: Modelling the physical impact of trawl components on the seabed and comparison with sea trials, Ocean Eng., 38, 925–933, https://doi.org/10.1016/j.oceaneng.2010.09.011, 2011.
- Jorgensen, B. B.: A comparison of methods for the quantification of bacterial sulfate reduction in coastal marine sediments, Geomicrobiol. J., 1, 11–27, 1978.
  - Jørgensen, B. B.: Sulfur biogeochemical cycle of marine sediments, Geochem. Perspect., 10, 145–146, 2021.
  - Kaiser, M. J., Collie, J. S., Hall, S. J., Jennings, S., and Poiner, I. R.: Modification of marine habitats by trawling activities: prognosis and solutions, Fish Fish., 3, 114–136, https://doi.org/10.1046/j.1467-2979.2002.00079.x, 2002.
- Kalapurakkal, H. T., Dale, A. W., Schmidt, M., Taubner, H., Scholz, F., Spiegel, T., Fuhr, M., and Wallmann, K.: Sediment resuspension in muddy sediments enhances pyrite oxidation and carbon dioxide emissions in Kiel Bight, Commun. Earth Environ., 6, 156, https://doi.org/10.1038/s43247-025-02132-4, 2025.
- Kallmeyer, J., Ferdelman, T. G., Weber, A., Fossing, H., and Jørgensen, B. B.: A cold chromium distillation procedure for radiolabeled sulfide applied to sulfate reduction measurements, Limnol. Oceanogr. Methods, 2, 171–180, https://doi.org/10.4319/lom.2004.2.171, 2004.
  - Krumins, V., Gehlen, M., Arndt, S., Van Cappellen, P., and Regnier, P.: Dissolved inorganic carbon and alkalinity fluxes from coastal marine sediments: model estimates for different shelf environments and sensitivity to global change, Biogeosciences, 10, 371–398, https://doi.org/10.5194/bg-10-371-2013, 2013.
- LaRowe, D. E., Arndt, S., Bradley, J. A., Burwicz, E., Dale, A. W., and Amend, J. P.: Organic carbon and microbial activity in marine sediments on a global scale throughout the Quaternary, Geochim. Cosmochim. Acta, 286, 227–247, https://doi.org/10.1016/j.gca.2020.07.017, 2020.
  - Łukawska-Matuszewska, K. and Dwornik, M.: Early diagenesis in anoxic sediments of the Gulf of Gdańsk (southern Baltic Sea): Implications for porewater chemistry and benthic flux of carbonate alkalinity, Front. Earth Sci., 13, 1593031, https://doi.org/10.3389/feart.2025.1593031, 2025.

- Martín, J., Puig, P., Masqué, P., Palanques, A., and Sánchez-Gómez, A.: Impact of Bottom Trawling on Deep-Sea Sediment Properties along the Flanks of a Submarine Canyon, PLoS ONE, 9, e104536, https://doi.org/10.1371/journal.pone.0104536, 2014.
  - Middelburg, J. J. and Levin, L. A.: Coastal hypoxia and sediment biogeochemistry, Biogeosciences, 6, 1273–1293, 2009.
- 970 Middelburg, J. J., Soetaert, K., and Hagens, M.: Ocean Alkalinity, Buffering and Biogeochemical Processes, Rev. Geophys., 58, e2019RG000681, https://doi.org/10.1029/2019RG000681, 2020.
  - Morys, C., Brüchert, V., and Bradshaw, C.: Impacts of bottom trawling on benthic biogeochemistry in muddy sediments: Removal of surface sediment using an experimental field study, Mar. Environ. Res., 169, 105384, https://doi.org/10.1016/j.marenvres.2021.105384, 2021.
- Oberle, F. K. J., Swarzenski, P. W., Reddy, C. M., Nelson, R. K., Baasch, B., and Hanebuth, T. J. J.: Deciphering the lithological consequences of bottom trawling to sedimentary habitats on the shelf, J. Mar. Syst., 159, 120–131, https://doi.org/10.1016/j.jmarsys.2015.12.008, 2016a.
  - Oberle, F. K. J., Storlazzi, C. D., and Hanebuth, T. J. J.: What a drag: Quantifying the global impact of chronic bottom trawling on continental shelf sediment, J. Mar. Syst., 159, 109–119,
- 980 https://doi.org/10.1016/j.jmarsys.2015.12.007, 2016b.
  - Olsgard, F., Schaanning, M. T., Widdicombe, S., Kendall, M. A., and Austen, M. C.: Effects of bottom trawling on ecosystem functioning, J. Exp. Mar. Biol. Ecol., 366, 123–133, https://doi.org/10.1016/j.jembe.2008.07.036, 2008.
- Palanques, A., Puig, P., Guillén, J., Demestre, M., and Martín, J.: Effects of bottom trawling on the Ebro continental shelf sedimentary system (NW Mediterranean), Cont. Shelf Res., 72, 83–98, https://doi.org/10.1016/j.csr.2013.10.008, 2014.
  - Porz, L., Zhang, W., and Schrum, C.: Natural and anthropogenic influences on the development of mud depocenters in the southwestern Baltic Sea, Oceanologia, 65, 182–193, https://doi.org/10.1016/j.oceano.2022.03.005, 2023.
- Porz, L., Zhang, W., Christiansen, N., Kossack, J., Daewel, U., and Schrum, C.: Quantification and mitigation of bottom-trawling impacts on sedimentary organic carbon stocks in the North Sea, Biogeosciences, 21, 2547–2570, https://doi.org/10.5194/bg-21-2547-2024, 2024.
- Pusceddu, A., Bianchelli, S., Martín, J., Puig, P., Palanques, A., Masqué, P., and Danovaro, R.: Chronic and intensive bottom trawling impairs deep-sea biodiversity and ecosystem functioning, Proc. Natl. Acad. Sci., 111, 8861–8866, https://doi.org/10.1073/pnas.1405454111, 2014.
  - Rabouille, C., Gaillard, J.-F., Tréguer, P., and Vincendeau, M.-A.: Biogenic silica recycling in surficial sediments across the Polar Front of the Southern Ocean (Indian Sector), Deep Sea Res. Part II Top. Stud. Oceanogr., 44, 1151–1176, https://doi.org/10.1016/S0967-0645(96)00108-7, 1997.
- Reithmaier, G. M. S., Johnston, S. G., Junginger, T., Goddard, M. M., Sanders, C. J., Hutley, L. B., Ho, D. T., and Maher, D. T.: Alkalinity Production Coupled to Pyrite Formation Represents an Unaccounted Blue Carbon Sink, Glob. Biogeochem. Cycles, 35, e2020GB006785, https://doi.org/10.1029/2020GB006785, 2021.
  - Rooze, J., Zeller, M. A., Gogina, M., Roeser, P., Kallmeyer, J., Schönke, M., Radtke, H., and Böttcher, M. E.: Bottom-trawling signals lost in sediment: A combined biogeochemical and modeling approach to early diagenesis in a perturbed coastal area of the southern Baltic Sea, Sci. Total Environ., 906, 167551,
- 1005 https://doi.org/10.1016/j.scitotenv.2023.167551, 2024.

Sala, E., Mayorga, J., Bradley, D., Cabral, R. B., Atwood, T. B., Auber, A., Cheung, W., Costello, C., Ferretti, F., Friedlander, A. M., Gaines, S. D., Garilao, C., Goodell, W., Halpern, B. S., Hinson, A., Kaschner, K., Kesner-Reyes, K., Leprieur, F., McGowan, J., Morgan, L. E., Mouillot, D., Palacios-Abrantes, J., Possingham, H. P., Rechberger, K. D., Worm, B., and Lubchenco, J.: Protecting the global ocean for biodiversity, food and climate, Nature, 592, 397–402, https://doi.org/10.1038/s41586-021-03371-z, 2021.

- Schönke, M., Clemens, D., and Feldens, P.: Quantifying the Physical Impact of Bottom Trawling Based on High-Resolution Bathymetric Data, Remote Sens., 14, 2782, https://doi.org/10.3390/rs14122782, 2022.
- Schroller-Lomnitz, U., Hensen, C., Dale, A. W., Scholz, F., Clemens, D., Sommer, S., Noffke, A., and Wallmann, K.: Dissolved benthic phosphate, iron and carbon fluxes in the Mauritanian upwelling system and implications for ongoing deoxygenation, Deep Sea Res. Part Oceanogr. Res. Pap., 143, 70–84, https://doi.org/10.1016/j.dsr.2018.11.008, 2019.
  - Sciberras, M., Parker, R., Powell, C., Robertson, C., Kröger, S., Bolam, S., and Geert Hiddink, J.: Impacts of bottom fishing on the sediment infaunal community and biogeochemistry of cohesive and non-cohesive sediments: Trawling impacts on ecosystem processes, Limnol. Oceanogr., 61, 2076–2089,
- 1020 https://doi.org/10.1002/lno.10354, 2016.
  - Slomp, C. P., Van Der Gaast, S. J., and Van Raaphorst, W.: Phosphorus binding by poorly crystalline iron oxides in North Sea sediments, Mar. Chem., 52, 55–73, https://doi.org/10.1016/0304-4203(95)00078-X, 1996.
- Sommer, S., Linke, P., Pfannkuche, O., Schleicher, T., Schneider V. D, D., Reitz, A., Haeckel, M., Flögel, S., and Hensen, C.: Seabed methane emissions and the habitat of frenulate tubeworms on the Captain Arutyunov mud volcano (Gulf of Cadiz), Mar. Ecol. Prog. Ser., 382, 69–86, https://doi.org/10.3354/meps07956, 2009.
  - Sommer, S., Gier, J., Treude, T., Lomnitz, U., Dengler, M., Cardich, J., and Dale, A. W.: Depletion of oxygen, nitrate and nitrite in the Peruvian oxygen minimum zone cause an imbalance of benthic nitrogen fluxes, Deep Sea Res. Part Oceanogr. Res. Pap., 112, 113–122, https://doi.org/10.1016/j.dsr.2016.03.001, 2016.
- Sommer, S., Dale, A. W., Bernsee, S., Domeyer, B., Gabriel, N., Kitte, A., Pankan, L., Okolski, S., Petersen, A., Subic, A., Kalapurakkal, H., and Türk, M.: Field-experiment to determine the short-term impact of bottom trawling on the benthic ecosystem in the German coastal Baltic Sea Cruise No. AL616, 18.07. 09.08.2024, Kiel (Germany) Kiel (Germany), MGF-OSTSEE-2024, GEOMAR, 2025.
  - Stephens, J. D. and McConnaughey, R. A.: Physical and geochemical responses to bottom trawling on naturally disturbed sediments in the eastern Bering Sea, ICES J. Mar. Sci., 81, 1512–1520,
- 1035 https://doi.org/10.1093/icesjms/fsae094, 2024.

- Tengberg, A., F De Bovee, P Hall, Berelson, W., Chadwick, D., Ciceri, G., Crassous, P., Devol, A., Emerson, S., Gage, J., Glud, R., Graziottini, F., Gundersen, J., Hammond, D., Helder, W., Hinga, K., Holby, O., Jahnke, R., Khripounoff, A., Lieberman, S., Nuppenau, V., Pfannkuche, O., Reimers, C., Rowe, G., Sahami, A., and Sayles, F.: Benthic chamber and profiling landers in oceanography A review of design, technical solutions and functioning, Prog. Oceanogr., 35, 253–294, 1995.
- Tiano, J., De Borger, E., Paradis, S., Bradshaw, C., Morys, C., Pusceddu, A., Ennas, C., Soetaert, K., Puig, P., Masqué, P., and Sciberras, M.: Global meta-analysis of demersal fishing impacts on organic carbon and associated biogeochemistry, Fish Fish., 25, 936–950, https://doi.org/10.1111/faf.12855, 2024.
- Tiano, J. C., Witbaard, R., Bergman, M. J. N., Van Rijswijk, P., Tramper, A., Van Oevelen, D., and Soetaert, K.: Acute impacts of bottom trawl gears on benthic metabolism and nutrient cycling, ICES J. Mar. Sci., 76, 1917–1930, https://doi.org/10.1093/icesjms/fsz060, 2019.
  - Tiano, J. C., Depestele, J., Van Hoey, G., Fernandes, J., Van Rijswijk, P., and Soetaert, K.: Trawling effects on biogeochemical processes are mediated by fauna in high-energy biogenic-reef-inhabited coastal sediments, Biogeosciences, 19, 2583–2598, https://doi.org/10.5194/bg-19-2583-2022, 2022.
- Tréguer, P. J. and De La Rocha, C. L.: The World Ocean Silica Cycle, Annu. Rev. Mar. Sci., 5, 477–501, https://doi.org/10.1146/annurev-marine-121211-172346, 2013.
  - Trimmer, M., Petersen, J., Sivyer, D., Mills, C., Young, E., and Parker, E.: Impact of long-term benthic trawl disturbance on sediment sorting and biogeochemistry in the southern North Sea, Mar. Ecol. Prog. Ser., 298, 79–94, https://doi.org/10.3354/meps298079, 2005.

- Van Dam, B., Lehmann, N., Zeller, M. A., Neumann, A., Pröfrock, D., Lipka, M., Thomas, H., and Böttcher, M. E.: Benthic alkalinity fluxes from coastal sediments of the Baltic and North seas: comparing approaches and identifying knowledge gaps, Biogeosciences, 19, 3775–3789, https://doi.org/10.5194/bg-19-3775-2022, 2022.
- Van Denderen, P. D., Bolam, S. G., Friedland, R., Hiddink, J. G., Norén, K., Rijnsdorp, A. D., Sköld, M., Törnroos, A., Virtanen, E. A., and Valanko, S.: Evaluating impacts of bottom trawling and hypoxia on benthic communities at the local, habitat, and regional scale using a modelling approach, ICES J. Mar. Sci., 77, 278–289, https://doi.org/10.1093/icesjms/fsz219, 2020.
  - van de Velde, S. J., Hylén, A., and Meysman, F. J. R.: Ocean alkalinity destruction by anthropogenic seafloor disturbances generates a hidden CO2 emission, Sci. Adv., 11, https://doi.org/10.1126/sciadv.adp9112, 2025.
- van de Velde, S., Van Lancker, V., Hidalgo-Martinez, S., Berelson, W. M., and Meysman, F. J. R.:

  Anthropogenic disturbance keeps the coastal seafloor biogeochemistry in a transient state, Sci. Rep., 8, 5582, https://doi.org/10.1038/s41598-018-23925-y, 2018.
  - Wallmann, K., Diesing, M., Scholz, F., Rehder, G., Dale, A. W., Fuhr, M., and Suess, E.: Erosion of carbonate-bearing sedimentary rocks may close the alkalinity budget of the Baltic Sea and support atmospheric CO2 uptake in coastal seas, Front. Mar. Sci., 9, 968069, https://doi.org/10.3389/fmars.2022.968069, 2022.
- Warnken, K. W., Gill, G. A., Dellapenna, T. M., Lehman, R. D., Harper, D. E., and Allison, M. A.: The effects of shrimp trawling on sediment oxygen consumption and the fluxes of trace metals and nutrients from estuarine sediments, Estuar. Coast. Shelf Sci., 57, 25–42, https://doi.org/10.1016/S0272-7714(02)00316-5, 2003.
- Watling, L., Findlay, R. H., Mayer, L. M., and Schick, D. F.: Impact of a scallop drag on the sediment chemistry, microbiota, and faunal assemblages of a shallow subtidal marine benthic community, J. Sea Res., 46, 309–324, https://doi.org/10.1016/S1385-1101(01)00083-1, 2001.
  - Yuan-Hui, Li and Gregory, Sandra: Diffusion of ions in sea water and in deep-sea sediments, Geochim. Cosmochim. Acta, 38, 703–714, 1974.
  - Zeebe, R. E. and Wolf-Gladrow, D.: CO2 in seawater: equilibrium, kinetics, isotopes, Elsevier, 2001.
- Zhang, W., Porz, L., Yilmaz, R., Wallmann, K., Spiegel, T., Neumann, A., Holtappels, M., Kasten, S.,

  Kuhlmann, J., Ziebarth, N., Taylor, B., Ho-Hagemann, H. T. M., Bockelmann, F.-D., Daewel, U., Bernhardt, L., and Schrum, C.: Long-term carbon storage in shelf sea sediments reduced by intensive bottom trawling, Nat. Geosci., 17, 1268–1276, https://doi.org/10.1038/s41561-024-01581-4, 2024.